Understanding the influence of cation and activator type/chemistry on the reaction kinetics and mechanical strength of liquid and powder silicate activated slag systems

by

Akash Dakhane

A Thesis Presented in Partial Fulfillment
of the Requirements for the Degree
Master of Science

Approved November 2013 by the
Graduate Supervisory Committee:

Narayanan Neithalath, Chair
Barzin Mobasher
Subramaniam Rajan

ARIZONA STATE UNIVERSITY

December 2013

ABSTRACT

The increased emphasis on the detrimental effects of the production of construction materials such as ordinary portland cement (OPC) have driven studies of the alkali activation of aluminosilicate materials as binder systems derived from industrial byproducts. They have been extensively studied due to the advantages they offer in terms of enhanced material properties, while increasing sustainability by the reuse of industrial waste and reducing the adverse impacts of OPC production. Ground granulated blast furnace slag is one of the commonly used materials for their content of calcium and silica species. Alkaline activators such as silicates, aluminates etc. are generally used. These materials undergo dissolution, polymerization with the alkali, condensation on particle surfaces and solidification under the influence of alkaline activators.

Exhaustive studies exploring the effects of sodium silicate as an activator however there is a significant lack of work on exploring the effect of the cation and the effect of liquid and powder activators. The focus of this thesis is hence segmented into two topics: (i) influence of liquid Na and K silicate activators to explore the effect of silicate and hydroxide addition and (ii) influence of powder Na and K Silicate activators to explore the effect of cation, concentration and silicates.

Isothermal calorimetric studies have been performed to evaluate the early hydration process, and to understand the reaction kinetics of the liquid and powder alkali activated systems. The reaction kinetics had an impact on the early age behavior of these binders which can be explained by the compressive strength results. It was noticed that

the concentration and silica modulus of the activator had a greater influence than the cation over the compressive strength.

Quantification of the hydration products resultant from these systems was performed via thermo gravimetric analysis (TGA). The difference in the reaction products formed with varying cation and silicate addition in these alkali activated systems is brought out. Fourier transform infrared (FTIR) spectroscopy was used to investigate the degree of polymerization achieved in these systems. This is indicative of silica and alumina bonds in the system.

Differences in the behavior of the cation are attributable to size of the hydration sphere and polarizing effect of the cation which are summarized at the end of the study.

ACKNOWLEDGEMENTS

It would not have been possible to compile this master's thesis without the help and support of so many people in so many ways, to only some of whom it is possible to give mention here.

First and foremost, I would like to thank my parents, brother and family who have always shown me their undeniable support not only throughout my academic career, but for anything and everything I've pursued, for which my mere expression of thanks does not suffice.

I would like to express my deep and sincere gratitude to my advisor, Dr. Narayanan Neithalath. I am extremely grateful and indebted to him for the expert, sincere and valuable guidance and encouragement he has extended to me throughout the learning process of this master's thesis. I also thank my thesis committee members, Dr. Subramaniam Rajan and Dr. Barzin Mobasher for consenting to examine my thesis.

I thank my lab mates Kirk, Ussala, Matt and Sateesh for all their help and discourse during the course of this work. Special thanks go to Kirk for his time and valuable comments while preparing this document.

Finally, I would like to give acknowledgment to Arizona State University School of Sustainable Engineering and the Built Environment for funding me as a research assistant which has allowed me to pursue my M.S. in Civil Engineering.

TABLE OF CONTENTS

CHAPTER Page

CHAPTER Page

CHAPTER Page

LIST OF TABLES

Table Page

LIST OF FIGURES

Figure Page

Figure Page

Figure Page

Figure Page

1. INTRODUCTION

The rapid growth in industrialization in the past decades has brought about the release of numerous undesirable pollutants into the atmosphere. Despite the diminishing availability of natural resources, the demand for portland cement based concrete has been ever increasing. Moreover, the manufacturing process of portland cement raises issues of energy consumed (requiring temperatures up to 1400-1500°C), along with the detrimental effects of the greenhouse gases such as CO_2, SO_2 etc. released in the environment. Alternative cementitious materials are an area of increasing interest due to growing environmental issues and the relatively large carbon footprint of the cement industry which accounts to approximately 5%. The construction industry has been using these byproducts, but only as fillers and not as a binding matrix. These concerns have led to studies of the alkali activation of aluminosilicate materials as sustainable binder systems which are derived from industrial byproducts. They are being studied extensively due to the advantages they offer in terms enhanced material properties, durability and sustainability by the reuse of industrial waste and byproducts and reducing the adverse impacts of OPC production. The most commonly used source materials of these aluminosilicate binders are slag, metakaolin, fly ash for their presence of soluble silica, calcium and alumina species. When mixed with highly alkaline activators, these materials undergo a dissolution mechanism followed by a polycondensation reaction to set and harden, delivering a material with very effective binding properties.

The source materials, activating alkali agent and the curing conditions are the most influential factors on the properties of the resulting product. The focus of this study

touches on all these aspects, by exploring the influence of binder composition (slag), the effect of the alkali cation (K or Na), the influence of silica to activator ratio and activator concentration in both liquid and powder activation.

Detailed experimental studies have been conducted to understand the early age properties and reaction kinetics of the binder. Reaction products formed in these systems have been characterized by means of advanced material characterization techniques, including FTIR and TGA. It is expected that an increased understanding of the properties of these systems facilitated through this study will provide stimulus for the increased use of cement-free binder concretes.

1.1 Objectives

The main objectives of this study are listed below:

i. To understand the effects of cation (Na and K) and the effect of externally added hydroxide in liquid alkali silicate and hydroxide activated slag and evaluate the reaction kinetics using isothermal calorimetry and compressive strengths and reaction product quantification and characterization techniques using thermo-gravimetric analysis, fourier transform infrared spectroscopy and NMR of cured alkali silicate and alkali hydroxide activated slag pastes;

ii. To understand the effects of cation (Na and K) in powdered alkali silicate and hydroxide activated slag used in terms of reaction kinetics, compressive strength, thermo-gravimetry and FTIR.

1.2 Thesis Layout

Chapter 2 provides a literature review of past studies on alkali activated binder systems. This will include a review on the reaction mechanisms of the alkali activated binders and their properties. It also provides a brief review on testing techniques used in the characterization of alkali activated binders.

Chapter 3 details the experimental design, including raw material properties, mixture proportions, mixing procedures and test methods used to assess the properties of the alkali activated slag systems.

Chapter 4 discusses the findings of the studies in the liquid alkali silicate activation of slag binder systems. The influence of cation and externally added hydroxide on the reaction kinetics, compressive strength and the reaction product formation and composition is studied in detail.

Chapter 5 is devoted to the understanding of the effect of the alkali cation used in the powder activation of slag binders. The difference in the reaction kinetics and mechanism when sodium and potassium silicates are used for the activation of these binders is brought out in this chapter.

Chapter 6 provides a detailed conclusion of the studies carried out on the alkali activated binder systems.

2. LITERATURE REVIEW

In this chapter the existing published work on the alkali activated slag with sodium silicate and hydroxide as activators is discussed.

2.1 Background and Overview

Ordinary Portland cement production leads to the production and expulsion of pollutants and various greenhouse gases into the environment (Marland et al., 1989; Taylor et al., 2006; Worrell et al., 2001). With the increased emphasize on environmental protection, whilst maintaining the rapid pace of infrastructural advance, it is necessary to investigate alternatives that do not cause detrimental effects onto the environment. The reduction of greenhouse gas emissions and minimizing the energy consumed to create materials used for infrastructure are amongst the goals for environmental conservation. In the last 100 plus years, ordinary portland cement (OPC) has become amongst the most profusely used commodities worldwide. This extensive use comes at a high cost to the environment, as the production of OPC requires very high temperatures (1400-1500°C) and thus a large amount of energy and emission of greenhouse gases due to both chemical reactions during production and energy use. The production of one ton of OPC releases approximately one ton of CO_2 (Mahasenan et al., 2003) and requires over 5000 MJ of energy (not including the energy required for quarrying raw materials)(Choate, 2003)

Another environmental concern is in regards to the consequences of improper waste disposal of industrial by-products, such as fly ash from coal burning for power generation and blast furnace slag from steel production. If unused, these industrial byproducts are deposited in landfills. Landfilling is generally undesirable due to the high costs and the

liability associated with the risk of contaminating ground water resources. In this context, industry has been looking for ways to recycle and reuse waste material as a better option to landfilling and disposing (Cheerarot and Jaturapitakkul, 2004).

To overcome these problems, investigations of the alkali activation of aluminosilicate materials as binder systems derived from industrial byproducts have emerged. They have been extensively studied due to the advantages they offer in terms enhanced material properties, while maintaining sustainability by the reuse of industrial waste by-products and reducing the adverse impacts of OPC production. Ground granulated blast furnace slag (GGBFS) is commonly used for their content of soluble silica and calcium species that can undergo dissolution, polymerization with the alkali, condensation on particle surfaces and solidification, providing the strength and stability of the binders. The resulting material was termed “geopolymers” by French scientist Joseph Davidovits in 1991.

Geopolymers can be used to bind loose aggregates together to form geopolymer concretes that can provide comparable performance to traditional cementitious binders in a range of applications with the added advantage of reducing greenhouse gas emissions and recycling industrial wastes (Duxson et al., 2007). Depending on the starting raw material and processing conditions, alkali activated binders can exhibit a wide assortment of properties and characteristics, including high compressive strength, low shrinkage, fast or slow setting, resistance against chemical attacks, fire resistance and low thermal conductivity (Duxson et al., 2007).

2.2 Geopolymer Theory

Geopolymerization is a geosynthesis, a reaction that chemically integrates minerals (Khale and Chaudhary, 2007), in which aluminosilicate materials such as fly ash and slag are exposed to high-alkaline environments in the form of hydroxides or silicates. The alkali component in the activator is a compound from the first group in the periodic table, such that geopolymers are also termed “alkali activated alumino-silicate binders”. These materials are characterized by a two- or three-dimensional Si-O-Al structure (McDonald and Thompson, 2003) , where silicon and aluminum atoms react to form molecules that are structurally and chemically similar to natural rocks.

These binders have since been classified into three groups:

i. Binders synthesized from materials with composition rich in calcium such as GGBFS that produces calcium alumino silicate hydrate (C-A-S-H) gel when activated with alkaline solutions (Alonso and Palomo, 2001) under normal curing conditions.
ii. Raw materials low in calcium and with high SiO_2 and Al_2O_3 contents such as fly ash. These materials modify into an amorphous material (alkaline aluminosilicate) that develops high mechanical strengths at early ages under thermal curing.
iii. Binders manufactured from a blend of raw materials from the previous two groups, Ca, Si and Al rich material (Palomo et al., 2007; Yip et al., 2005)

The reaction mechanisms of these materials differ significantly from OPC. Pozzolanic cement relies on the presence of calcium in the form of C-S-H gel for matrix and strength

development, whereas geopolymers utilize the polycondensation of the silica and alumina precursors and a high alkali content to achieve structural strength (van Jaarsveld et al., 2002).

2.2.1 Development of Aluminosilicate Binders

In order to examine the molecular structures of alkali activated binders or cement-free binders the term polysialate was coined as a descriptor of the silico-aluminate structure for this type of material. The network is configured of SiO_4 and AlO_4 tetrahedrons united by oxygen bridges (Figure 1), which has often been described to be similar to a sodalite network (Davidovits, 1999). Due to the negative charge of the Al tetrahedral in IV-fold coordination, positive ions must be present to balance out this charge. These ions (Na^+, K^+) must compensate the negative charge which is the reason why alkali silicates or hydroxides are used as the activating agents.

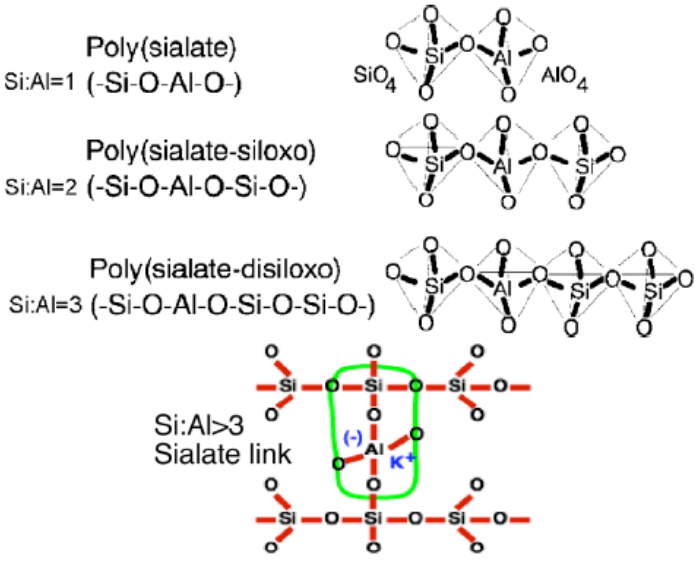

Figure 1**:** Aluminosilicate Structure and Nomenclature (Davidovits, Geopolymer, Green Chemistry and Sustainable Development Solutions, 2005)

A Ukrainian research, Glukhovsky (Glukhovsky, 1959) in the 1950s offered a general representation of the mechanism for the alkali-activation of compromising of silica and alumina species, which he termed as "soil-cements" in 1960s (Glukhovsky, 1965). Glukhovsky's model primarily divided the process into three distinct steps: (a) destruction-coagulation; (b) coagulation-condensation; (c) condensation-crystallization. Since then, different authors have elaborated on and extended Glukhovsky's theories with the added application of knowledge about zeolite synthesis.

Davidovits took this forward expressing the reaction leading to the formation of a polysialate geopolymer (Davidovits, 1999) as shown below:

$$(Al_2Si_2O_7)_n + nH_2O \xrightarrow{MOH} n(OH)_3 - Si - Al - (OH)_3 \qquad \textbf{(2.2.1-1)}$$

$$n(OH)_3 - Si - O - Al - (OH)_3 \xrightarrow{MOH} M\left(\begin{array}{c} | \\ -Si - O - Al^{(-)} - O \\ | \quad\quad | \\ O \quad\quad O \end{array}\right)_n + nH_2O \qquad \textbf{(2.2.1-2)}$$

In the above equations, *M* is the activation cation used in the reaction which is generally introduced as either KOH or NaOH. Additional amounts of amorphous silica must be present in order to form either the polysialate-siloxo or polysialate-disiloxo structures of geopolymers. The reaction for the polysialate-siloxo formation is also provided below as an illustration of how the two reactions differ (Davidovits, 2005).

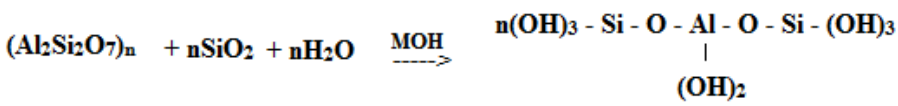

(2.2.1-3)

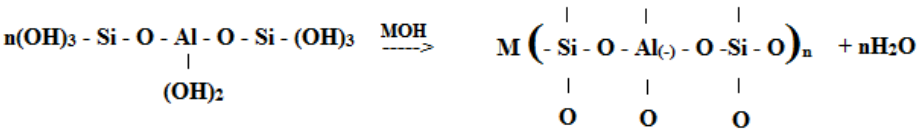

(2.2.1-4)

After the geopolymerization process is completed, the final geopolymer obtained is described by the empirical formula:

(2.2.1-5)

$$\mathbf{M_n\{-(SiO_2)z-(AlO_2)\}n + H_2O}$$

Here *M* again is a cation used to activate the reaction, n is the degree of polycondensation, and *z* = 1, 2, 3 for polysialate, polysialate-siloxo, and polysialate-disiloxo structures respectively.

Figure 2 below illustrates a simplified model of the polymerization process of alkali-activated geopolymers as they transform from a solid aluminosilicate source into a synthetic alkali aluminosilicate.

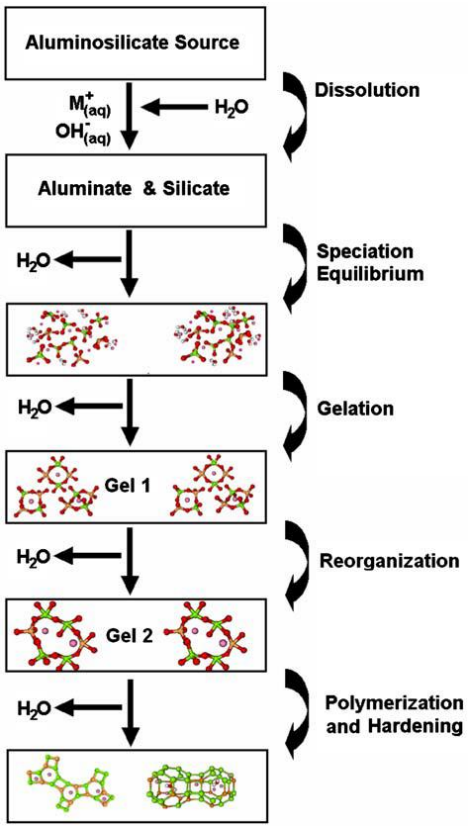

Figure 2: Conceptual model for geopolymerization process (Duxson, et al 2007)

Dissolution of the solid aluminosilicate source by the alkaline hydrolysis produces aluminate and silicate species (Duxson et al., 2007). It occurs immediately upon contact between the alkaline activating solution and aluminosilicate source material, allowing for an ionic interface between species and breaking the covalent bonds to liberate the silicon, aluminum and oxygen atoms (Saeed et al., 2010). Similar to OPC reactions, this step usually generates rapid and intense heat (as shown in isothermal calorimetric data in Chapter 3), and is directly proportional to the pH level and concentration of the activating solutions. The rate of the dissolution step is also a function of the amount and

composition of the source material and pH of the activating solution (Fernández-Jiménez et al., 2006).

Once dissolution is complete, the species released are incorporated into the aqueous phase, which may already contain free silicate from the activating solutions, providing a complete mixture of silicate, aluminate and aluminosilicate species. With activating solutions with a high pH, the dissolution is rapid and creates a supersaturated aluminosilicate solution. When the concentration reaches a substantial level, a gel starts to form as the oligomers in the aqueous phase form large networks consisting of Si-O-Al-O bonds through condensation. At this stage, water that was consumed during dissolution is released and plays the role of a reaction facilitator, residing within the pores of the gel. The formed gel is initially aluminum-rich and contains alkaline cations that compensate for the deficit charges produced with the aluminum-for-silicon substitution (Saeed et al., 2010).

After gelation, the system continues to rearrange and reorganize as the connectivity of the gel network increases, resulting in a three-dimensional aluminosilicate network, as represented in Figure **2** with the presence of multiple "gel stages" (Duxson et al., 2007).

2.2.2 Alkaline Activation of Ground Granulated Blast Furnace Slag (GGBFS)

Ground Granulated Blast Furnace Slag (GGBFS) is an industrial by-product of the smelting ore process, which is used to separate the desired metal fraction from the unwanted fraction. It is usually comprised of metal oxides and silicon dioxide, but can also contain metal sulfides and pure metal atoms in their elemental form. The alkali-activation of blast-furnace slag has been used as an alternative to cement in concrete

production for over 65 years (Altan and Erdoğan, 2012; Purdon, 1940; Roy, 1999). Alkalis initially attack the outer layer of the slag particles, breaking them up until ultimately a polycondensation of reaction products occurs. An initial stage of reaction products form during dissolution and precipitation, but at later stages a solid state mechanism takes place on the surface of the formed particles which is dominated by slow diffusion of the ionic species into the virgin core (Chithiraputhiran, 2012). In this reaction, the alkali cations (M^+) acts as a catalyst for the reaction in the initial stages of hydration as shown in the following equations, where the cations are exchanged with free Ca^{2+} ions (Glukhovsky et al., 1980; Krivenko, 1994):

$$\mathbf{=Si\text{-}O^- + M^+ \rightarrow =Si\text{-}O\text{-}M} \qquad \mathbf{(2.2.2\text{-}1)}$$

$$\mathbf{=Si\text{-}O\text{-}M + OH^- \rightarrow =Si\text{-}O\text{-}M\text{-}OH^-} \qquad \mathbf{(2.2.2\text{-}2)}$$

$$\mathbf{=Si\text{-}O\text{-}M\text{-}OH^- + Ca^{2+} \rightarrow =Si\text{-}O\text{-}Ca\text{-}OH + M^+} \qquad \mathbf{(2.2.2\text{-}3)}$$

As is evident, the alkaline cations perform as structure creatures. The nature of the anions also plays a role in activations, particularly at early ages in regards to paste setting (Fernández-Jiménez et al., 2003; Puertas and Fernández-Jiménez, 2001).

The final reaction products obtain are similar to those of OPC hydration (C-S-H gel), with the distinction being the rate and intensity of the reaction. Since slag contains reactive silica, it also exhibits pozzolanic activity in the presence of calcium hydroxide. Thus, when blended with OPC, there will be three distinct steps: cement hydration, slag hydraulic reaction and slag pozzolanic activity (Ravikumar and Neithalath, 2012a).

2.3 Alkaline Activators and Their Properties

The activation of the selected binder materials contributes the most significantly in producing a structurally sound material via the geopolymeric process. It is the activator that prompts the dissolution, precipitation and crystallization of the aluminosilicate species. When using hydroxides, the OH^- acts as a catalyst for the reaction and the metal cation (Na^+ or K^+) serves as a charge balance for the aluminum framework. The initial steps of the alkali activation reaction process is thus dependent on the alkaline solutions ability to dissolve the source binder material and release reactive silicon and aluminum into solution (Saeed et al., 2010).

The alkaline solutions are derived using soluble alkali metals that are usually sodium or potassium based. The most common alkaline liquid used in geopolymerization is a combination of sodium hydroxide (NaOH) or potassium hydroxide (KOH) and sodium silicate ($Na_2O{\cdot}nSiO_2$) or potassium silicate ($K_2O{\cdot}nSiO_2$) (Hardjito and Rangan, 2005).

2.3.1 Alkali Hydroxides as activating agents

The most commonly used activators are hydroxides of sodium (NaOH) and potassium (KOH). Since K^+ is more basic it provides a higher degree dissolution and polymeric ionization of the source material, leading to denser polycondensation reaction and more enhanced matrix formation. However, higher concentrations of KOH have been shown to decrease the resulting compressive strength due to excessive K^+ ions in the solution and leaching of Si/Al occurring excessively (Khale and Chaudhary, 2007).

While KOH is generally found to achieve greater degrees of dissolution, NaOH actually has a greater ability to liberate silicate and aluminate monomers. This is due to sodium cations being much smaller than potassium cations and can migrate throughout the paste network, thus promoting better zeolitization (Rangan, 2008).

2.3.2 Alkali Silicates as activating agents

Sodium (or potassium) silicates are manufactured by fusing sand (SiO_2) with sodium or potassium carbonate (Na_2CO_3 or K_2CO_3) at temperatures ranging from 1100-1200°C and subsequently dissolved with high pressure steam into a clear, semi-viscous fluid known as "waterglass" (McDonald and Thompson, 2003). However, waterglass is rarely ever used as an independent activating solution since it does not contain the required activation potential to initiate the geopolymeric process on its own. Instead, it is often mixed with an alkali hydroxide solution to enhance its alkalinity to ensure increased specimen strengths.

The ratio of silicate and hydroxide plays an important role on the compressive strength development of the resulting specimen. In general, an increase in the concentration of the alkali (or decreasing the added soluble silicate) results in an increase of the compressive strength. This is because an excess of soluble silicates retards water evaporation and structure formation (Khale and Chaudhary, 2007). Thus, care must be taken to regulate the ratio between hydroxides and silicates.

2.4 Synthesis of Alkali Activated Binders

The production of a cement-free binder requires source material rich in aluminum and silicate species as the binder, alkali solutions for activation, and certain types of source material necessitate the application of heat curing to obtain reasonable mechanical properties.

2.4.1 Common mixing procedures

The principal difference between a geopolymer concretes and OPC concretes is in the binder paste. A geopolymer requires the addition of an alkali activator to react with the silicon and aluminum oxides in order for hydration to occur, binding loose aggregates together to form the geopolymer concrete.

Studies have also found that when the source material contains calcium (such as slag or Class C fly ash), the setting of the mixture is low and handling of the mixture is difficult due to early stiffening (Astutiningsih and Liu, 2005). This phenomena is more prevalent for systems activated with Na^+ cations than K^+ cations, since potassium has a better ability to dissolute and are also slightly less exothermic (as will be evident in later chapters).

2.4.2 Reaction Kinetics Evaluation

The hydration of ordinary portland cement binders is in general a five step process of dissolution, induction, acceleration, deceleration and finally diffusion limited. This evolution can be qualitatively characterized by the heat evolution sketch shown in Figure 3. The major activity during each stage is described as follows:

1. Pre-induction (Dissolution) – This is the initial rapid hydration that occurs when the particles of cement are exposed to water, releasing a large amount of heat. Duration: On the order of minutes.
2. Induction (Dormant) – A period of reduced hydration activity that allows for the transportation and placement of the mix. Duration: On the order of 1-2 h.
3. Acceleration – The rate of hydration increases. This is the beginning of the period during which the cement paste will achieve initial set. The major portion of the silicates hydrates and the cement solidifies. Duration: On the order of several hours.
4. Deceleration – The hydration rate decreases as the hydrated material covers the particles. Duration: On the order of hours to days.
5. Diffusion Limited – Hydration and aggregation occur at a very low rate. Reactions are limited by the rate of diffusion of species through the dense pore network. Duration: On the order of years (Bentz et al., 1994).

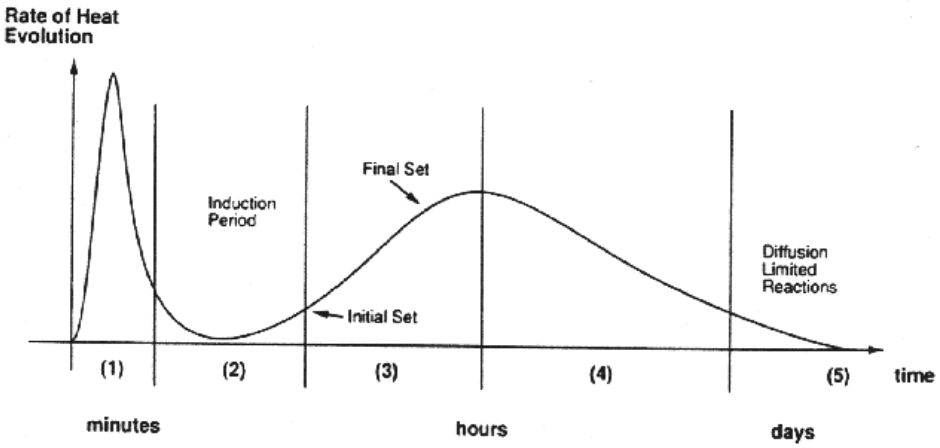

Figure 3: Heat evolution curve of cement hydration (Nelson, 1990)

In alkali activated systems with a calcium source, the primary reaction product is C-S-H with a low Ca/Si ratio. Its reaction kinetics is governed by the activator type, temperature and the alkalinity of the activator. In potassium silicate powder activated systems, the heat evolution response is similar to that of OPC hydration, as shown in Figure 3. The development of the peaks seems to have a direct relationship with the alkali concentration, with the time of occurrence decreasing with a decrease in alkali concentration.

It has been established that the initial pH of the activator plays a vital role in the initial dissolution of the binder and promoting the initial formation of hydration products. There are three models offered to describe the hydration of alkali activated slag cements. The first model describes the case where there is only one initial peak and no further peaks. The second model comprises of one peak before and after the dormant period, and finally the third model includes two peaks before the dormant period and one peak after (Shi & Day, A calorimetric study of early hydration of alkali-slag cements, 1995). The

potassium silicate powder activated systems follow the trends of the second model, which is the most akin to ordinary portland cement systems. For sodium silicate powder activated binders, the reaction takes place so quickly that the dissolution and accelerate periods are combined with no induction period recorded (similar to the first model). There has not been much research on the case of powder activated systems, which will be the focus of the research in Chapter 5.

2.5 Reaction product and microstructure analysis

2.5.1 Fourier Transform Infra-Red (FTIR) Spectroscopy analysis

Fourier Transform Infra-Red (FTIR) Spectroscopy is a quick and easy method for analyzing the reaction products formed in alkali activated binder systems. In infrared spectroscopy, infrared radiation is passed through a sample, where a portion of the radiation is absorbed and a portion is transmitted. The resulting spectrum represents the molecular absorption and transmission, creating a molecular fingerprint of the sample. This makes infrared spectroscopy useful for identification (qualitative generally, but quantitative also possible) of reaction products in these systems. Table 1 shows the common FTIR spectra peaks identified from literature for OPC and alkali activated pastes.

Table 1: Attributing FTIR peak signals to typical bonds (Yu et al. 1999)

Peak location (cm^{-1})	**Chemical bond characteristic of the signal**
3650	Hydrated Minerals (i.e. Ca(OH)2)
3600-3100	S-O (Gypsum)
3400	OH Stretching (H2O)
2930, 2850	Calcite Harmonic
1650	S-O (Gypsum) H-O-H Bending (H2O)
1430	C-O Asymmetric Stretching
1100	S-O (Gypsum) Si-O-Si and Al-O-Si Asymmetric Stretching
1035-1030	aluminosilicate bonding'
1010-1000	Calcium Silicates
960-800	Si-O, Al-O Stretching
872	C-O Bending
480	Si-O-Si and O-Si-O Bending

3. MATERIALS, MIXTURE PROPORTIONS AND TEST METHODS

The purpose of this chapter is to describe the materials used and the methodology employed for the research presented in this thesis. The experimental procedures used to create the samples are also explained in detail, along with a description of the equipment utilized for the analysis.

3.1 Materials

The binder materials used in this study are Class F fly ash conforming to ASTM C 618 and ground granulated blast furnace slag (GGBFS) Type 100 conforming to ASTM C 989, the chemical compositions of which are shown in

Table 2. The reactivity of these materials when activated with alkalis is predominantly dependent on the CaO, SiO_2 and Al_2O_3 contents of the binders. Figure 4 presents the CaO-SiO_2-Al_2O_3 ternary diagram indicating the location of the source materials by composition.

Table 2: Chemical composition and physical characteristics of slag

Chemical Analysis	**Slag**
Silicon Dioxide (SiO_2)	39.44%
Aluminum Oxide (Al_2O_3)	6.88%
Iron Oxide (Fe_2O_3)	0.43%
Calcium Oxide (CaO)	37.96%
Sulfur Trioxide (SO_3)	2.09%
Loss on Ignition (L.O.I)	3.00%
Sodium Oxide (Na_2O)	1.67%
Others	8.53%
Density (g/cc)	2.9

All three of these binding materials are silica and alumina rich, which are necessary for the formation of the strength imparting phases in alkali activated binders. The silica-to-alumina ratios were found to be approximately 2.48, 2.59 and 5.73 for the fly ashes and slag used. In addition to the high silica and alumina content in slag, it also contains a high CaO content (~38%), while the CaO content in Class F fly ash is very low (5.03 %) as expected.

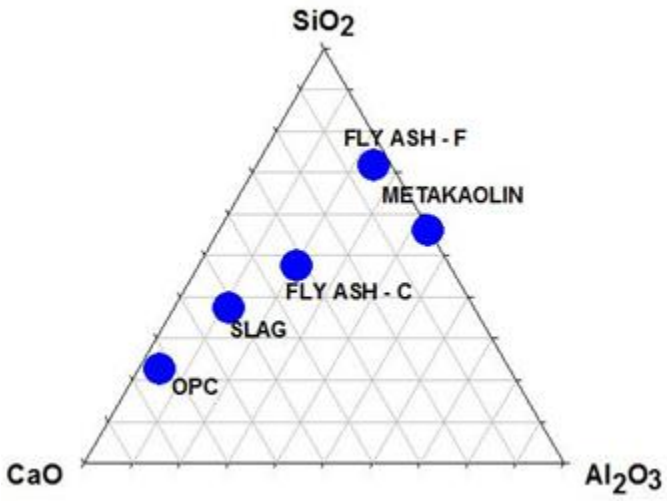

Figure 4: Ternary diagram illustrating the CaO-SiO_2-Al_2O_3 composition of different materials used in concrete production (Chithiraputhiran S. , 2012)

The particle size distributions of the fly ash and slag (obtained using a laser particle size analyzer) are shown in Figure . The particle size analysis indicates that slag is finer than fly ash with 95% of particles finer than 30 μm compared to only 60% for fly ash.

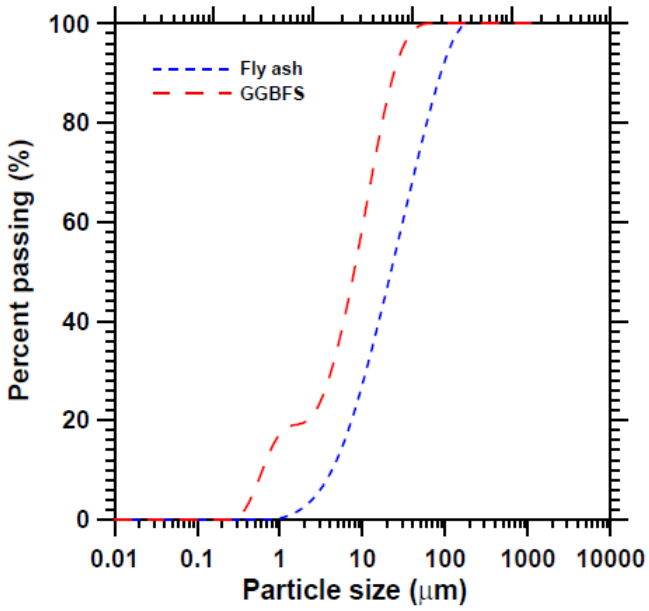

Figure 5: Particle size distribution of fly ash and slag (Ravikumar, Property Development, Microstructure and Performance of Alkali Activated Fly Ash and Slag Systems, 2012)

Slag particle morphologies obtained using scanning electron microscopy is shown in Figure 6. Slag is composed of angular particles of varying sizes.

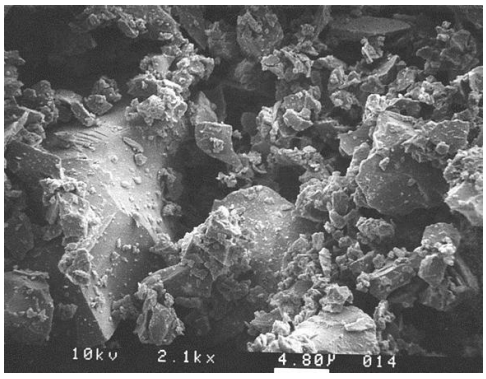

Figure 6: Scanning electron micrograph of slag (PCA, 2003)

3.2 Activator Parameters (M, *n* and M_s)

The activation parameters used in this study are the Na_2O-to-binder ratio (*n*) and the SiO_2-to-M_2O ratio (known as the silica modulus, M_s), and the solution concentration in terms of molarity (M) for alkali hydroxide activating solutions. The binders comprise of slag. The ratio *n* provides the total amount of M_2O (where M is either Na of K) in the mixture, while the M_s dictates the proportion of MOH and alkali-silicates in the activator. Thus, the total alkali contents are adjusted using the *n* parameter, for which several values were used in Chapter 5.

The activating agents used in Chapter 4 were two different sodium silicate (E-sodium silicate & D-sodium silicate), potassium silicate solutions (Kasil), sodium hydroxide and potassium hydroxide solutions whose details are given in Table 3-2. In Chapter 5, powder activators were used in the form of potassium silicate (Kasolve) or GD-sodium silicate (GDSS) with a molar M_s of 2.51 and 3.32 respectively. Since previous studies have shown that such high M_s values are not effective in activation of fly ashes (Chithiraputhiran and Neithalath, 2013; Ravikumar and Neithalath, 2012a), reagent grade NaOH or KOH were added to the alkali-silicates to reduce their M_s values.

For example, if a mixture containing 1000g of binders was to be prepared with an *n* value of 0.05 and an M_s of 1.5, 50 g of Na_2O and 72.58 g of SiO_2 will be required. If sodium silicate with 36.3% solid's content is used as the source of silica in the activator solution, 72.58 g of SiO_2 can be acquired using 262 g of waterglass, which contains 95.12 g of dissolved sodium silicate powder with a mass-based M_s ratio of 3.22. The sodium silicate also provides 22.5 g of Na_2O, and the remaining 27.4 g will be obtained with the addition

of NaOH. Table 3 shows the mixture proportions used for 1000 g of binders with the activation parameters *n* of 0.05 with different M_s ratios (1.0, 1.5, 2.0 and 2.5). A water-to-powder ratio (w/p) of 0.4 was used, where the water consisted of the water added, the water proportion of silicate and water generated in the dissociation of the alkali-hydroxide. The powders consisted of the binders, the solid fraction of silicate solution and the M_2O from MOH.

Table 3: Sample mixture proportions of liquid activators for 1000g of slag for *n* values of 0.05, and M_s values of 1.0, 1.5, 2.0 and 2.5

Activator solutions	Na-Si (M_s = 3.3, 36%)			Na-Si (M_s = 2.0, 44%)			K-Si (M_s = 3.3, 36%)		
M_s	1	1.5	2.5	1	1.5	2	1	1.5	2.5
Na/K silicate solution(g)	174	262	436	164	246	340	130	196	327
NaOH/KOH (g)	45	35	16	33	17	0.0	41	32	14
Water (g)	317	274	186	339	307	269	342	308	240

Table 4: Sample mixture proportions of powder activators for 1000g of slag for *n* values of 0.05, and M_s values of 1.0, 1.5 and 2.0

Activator powder	Na-Si (M_s = 2.0)			K-Si (M_s = 2.5)		
M_s	1	1.5	2	1	1.5	2
Na/K silicate powder(g)	72	108	145	51	77	103
NaOH/KOH (g)	33	17	2.	35	23	12
Water (g)	431	445	458	427	435	443

The powder activated samples were prepared a similar way as shown in Table 4; however the liquid consisted only of added water and water generated in the dissociation of the alkali-hydroxide.

3.3 Mixing Procedure

3.3.1 Liquid activated systems

In the liquid activated systems using sodium silicate the NaOH solution used to reduce the activator M_s was prepared by dissolving in water and added to the required amount of water glass. For NaOH activated samples, the required amount of NaOH was first weighed into a measuring cylinder into which the required volume of water was added. For both cases resulting solution was then allowed to cool down to the room temperature. A w/p ratio of 0.4 was used for all silicate activated systems.

River sand (d_{50} of 0.6 mm) was used as the fine aggregate. The mortar mixtures were proportioned to contain a sand volume of approximately 44±2%. Fly ash and the fine aggregates were dry-mixed thoroughly in a laboratory mixer. Requisite amount of the alkaline activator solution of the chosen concentration was gradually added while mixing until the components were homogenized. The mortar was filled in cubical acrylic molds of 2 inches size, and compacted using a table vibrator. Corresponding paste mixtures were also prepared for thermal analysis and spectroscopic studies.

3.3.2 Powder activated systems

In the powder activated systems using Kasolv and GDSS, a sand volume of 44±1% was used as the fine aggregate. The activator was prepared in the similar manner and the powder activators was added to water along with hydroxides and was allowed to cool down to ambient temperature. The calculated amounts of slag and fine aggregate were dry-mixed thoroughly in a laboratory mixer. The activator was then added to the starting materials to prepare the mortars and mixed for approximately 2 minutes until a

homogenous mixture is obtained. The mixtures were then cast in 50 mm cube molds for compressive testing and porosity measurements. Corresponding paste mixtures were also prepared for spectroscopic and calorimetric studies with a w/p ratio of 0.4.

3.4 Moist curing

For binders containing a calcium source (slag or fly ash-slag blends), the samples were subjected to moist curing at 23±2 °C and a relative humidity > 98%. The samples were covered in plastic prior to placing in the moist curing chamber to prevent ponding on the surface of the samples.

3.5 Early Age Tests

3.5.1 Isothermal Calorimetry

Isothermal calorimetry has been found to be a useful technique to investigate the hydration of cementitious systems (Wadsö, 2003). Isothermal calorimetry is typically used to investigate the main hydration peak that occurs during the acceleration phase of the hydration process. The experiments in this study were carried out in accordance with ASTM C 1679 using a Calmetrix ICal 8000 isothermal calorimeter. The paste mixtures were prepared using the same methods described in Section 3.3 and poured into the cups at constant mass (100 g) immediately before they were loaded into the isothermal calorimeter. The time elapsed between the water addition and sample loading was approximately 2 minutes. The tests were run for 72-96 hours with the calorimeter temperature set to 25°C. Figure shows the isothermal calorimeter used for this study.

Figure 7: Calmetrix ICal 8000 Isothermal Calorimeter

3.6 Hardened Mortar Tests

3.6.1 Determination of Compressive Strength

The compressive strengths of the pastes and mortars were determined in accordance with ASTM C 109. The compressive strengths of the alkali activated cubes at several ages were determined by testing at least three specimens from each mixture at the desired ages of 1, 3, 14, 28 and 56 days. Moist-cured specimens were tested at the respective ages after a few hours of drying at ambient conditions.

3.7 Reaction Product Analysis

3.7.1 Attenuated Total Reflectance - Fourier Transform Infrared Spectroscopy

Attenuated total reflectance – Fourier Transform Infrared Spectroscopy (ATR-FTIR) allows for the determination of transmission spectra without destructive sample preparation. Spectra are obtained from the absorption or transmittance of a wave which is transmitted through an internal reflection element (IRE) of high refractive index and penetrates a short distance into the sample, in contact with the IRE. The IRE used is a diamond, selected because of its resistance to high pH and abrasion from sample removal and cleaning. A picture of the ATR attachment along with a schematic diagram of the beam path through the apparatus is shown in Figure 8.

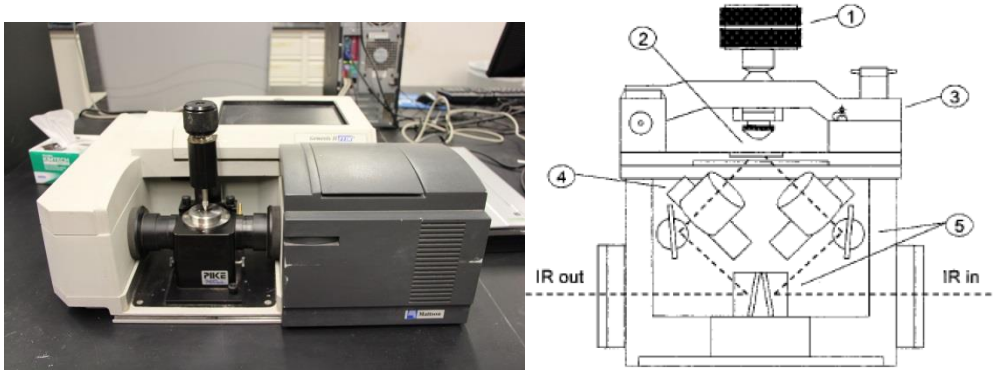

(a) **(b)**

Figure 8: a) ATR attachment with diamond crystal, (b). Schematic diagram showing the beam path through the ATR (1) torque head screw with limiter screw; (2) ATR crystal, (3) clamp bridge, (4) lens barrel, (5) mirrors

3.7.2 Thermogravimetric Analysis

Thermogravimetric analysis (TGA) is a useful laboratory tool used for material characterization. It is a technique in which the mass of a substance is monitored as a function of temperature or time as the sample specimen is subjected to a controlled

temperature program in a controlled atmosphere (PerkinElmer, 2010). The basic principle of TGA is that as a sample is heated, its mass changes. This change can be used to determine the composition of a material or its thermal stability, up to 1000°C. Usually, a sample loses weight as it is heated up due to decomposition, reduction, or evaporation. A sample could also gain weight due to oxidation or absorption. The TGA equipment tracks the change in weight of the sample via a microgram balance. Temperature is monitored via a thermocouple. TGA data is usually graphed as weight percent vs. temperature (°C). TGA output curves can be analyzed in a number of ways. If the material in question is stoichiometric, the molar weight of the component being burned off can be ascertained based on the weight percent lost and the total molar weight of the material. TGA was carried out on representative samples using the Perkin Elmer STA 6000. A heating rate of 15°C/min, and a temperature range from ambient to 995^{o}C was used for the thermal analysis studies. A picture of the TGA equipment used in this study is shown in Figure .

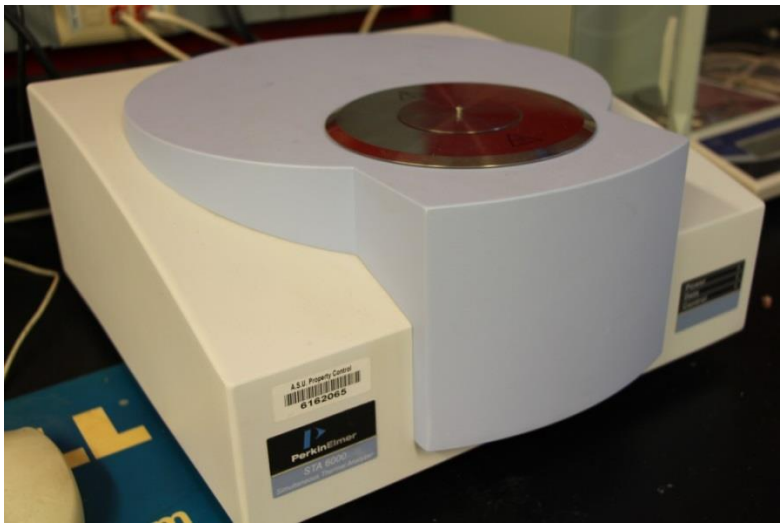

Figure 9: TGA equipment set up

4. INFLUENCE OF CATION AND EXTERNALLY ADDED HYDROXIDE ON LIQUID ALKALI SILICATE AND HYDROXIDE ACTIVATED SLAG

This chapter explores the influence of cation and the externally added hydroxide on the reaction kinetics, mechanical properties and degree of polymerization of the reaction product formed.

4.1 Isothermal Calorimetry of slag pastes

4.1.1 Influence of cation

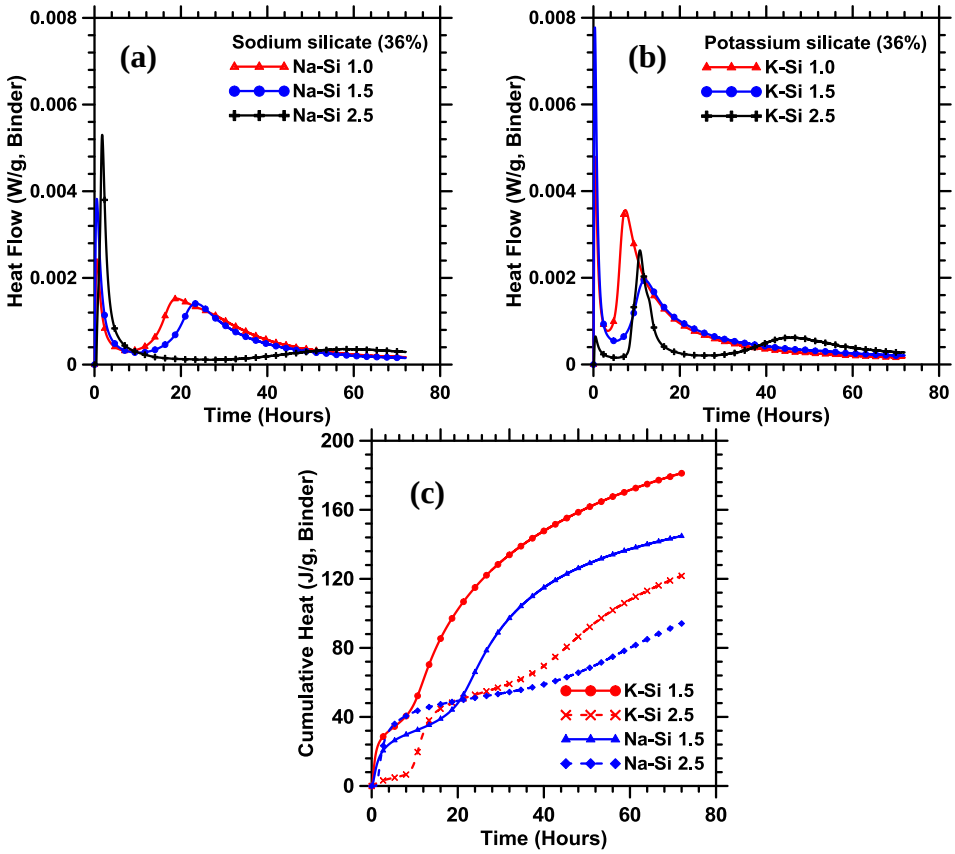

Figure 10: Heat evolution of slag pastes activated using (a) Na-silicate and (b) K-silicate, and (c) cumulative heat release at 25^{o}C after 72 h of reaction

Figure 10 shows the heat evolution of sodium and potassium silicate activated slag pastes respectively, proportioned using an n value of 0.05 and three different M_s values (1, 1.5

and 2.5). The as-obtained Na- and K-silicate activators with 36% solids content were used here, and NaOH or KOH solution was added to reduce the M_s values. In general, two distinct peaks appear as the result of reaction of slag with the alkaline solution – an initial dissolution peak and a later acceleration peak, similar to the heat release signature of OPC systems. The initial peak noticed during the first few hours is caused by particle wetting and the dissolution of the slag particles in the highly alkaline activator (Ravikumar and Neithalath, 2012a; Shi and Day, 1995). The Ca-O bonds and some amount of Al-O and Si-O bonds in slag are broken by the highly alkaline solution. Since external mixing was adopted, the dissolution peak magnitudes would not be accurate, even though they can be used for comparative purposes (Ravikumar and Neithalath, 2012b). The setting times of all the activated slag pastes studied here are relatively short, indicating the formation of insoluble reaction products around the slag particles. Higher M_s values of the activator induces more precipitation of Ca-containing reaction products early on but in the absence of large amounts of alkali cations, the polysilicate ion linkages are soluble in water (Vail and Wills, 1952). This explains the general increase in the heat release rate associated with dissolution as the activator M_s increases, and the subsequent delay in the acceleration peak. The dormant period after the dissolution peak is followed by the acceleration peak that corresponds to the strength-imparting reaction product formation in these systems. In systems with high alkalinity (lower values of M_s), the dormant period is relatively short as observed from these figures, attributable to the fact that the dissolution rates are enhanced and the ionic diffusion through the reaction product layer over the slag particles is enhanced. For the paste activated using K-silicate of M_s = 2.5 alone, there are two heat release signatures corresponding to the initial

reaction stage. While the first, smaller peak corresponds to the particle wetting and dissolution (higher M_s, and therefore reduced degree of dissociation), the second larger peak at around 12h could be attributed to the reaction between the dissolved Ca^{2+} in solution and the silicate anions from the activator (Chen and Brouwers, 2007). This effect is not noticed for the pastes activated using Na-silicates or when the activator M_s is decreased. When the M_s is lowered through the addition of alkali hydroxides, the initial dissolution rate is enhanced for both Na- and K-silicate activated mixtures, with a consequent precipitation of an insoluble, low Ca/Si molar ratio product (Al-rich gel). There is a higher amount of OH^- ions in solution to break further Si-O and Al-O bonds to react with Ca ions to form the C-(A)-S-H gel in these cases. For the same M_s value (of 2.5, here), the Na-silicate activated paste does not demonstrate the two initial peak behavior. This could be attributed to the K^+ ion being able to retain the soluble silicate anions stable for longer durations as compared to the Na^+ ion (Fernández-Jiménez et al., 2013). These anions react with the dissolved Ca^{2+} to form the second initial peak. Notice that a weak acceleration peak appears only at about 48h for this system that is much less alkaline because of the lower M_s.

For both the Na- and K-silicate activated pastes, decreasing the M_s (increasing alkalinity) increases the magnitude of the acceleration peak. The pastes proportioned with an M_s of 2.5, for both the silicate solutions, show extremely delayed and wide acceleration peaks of smaller magnitude. This is a result of the lower levels of alkalinity in these pastes, which consequently reduces the ability of the ions to penetrate the initially formed reaction product layer as described earlier (Ravikumar, 2012). The dormant period is found to be shorter for the K-silicate activated pastes as compared to the Na-silicate

activated pastes at the same M_s. The K-silicate activated pastes also demonstrate increased intensities of the acceleration peak, and a higher rate of the acceleration phase of the reaction as evidenced by the slope of the acceleration curve. The alkalinity of the activator solutions in these systems is significant, as high alkalinity favors better dissolution of the silica and alumina species in the binder and the formation of reaction products (Depasse, 1999, 1997). The smaller ionic radius of the solvated K^+ ion (Bach et al., 2013; Khale and Chaudhary, 2007; Provis and van Deventer, 2007) likely results in a faster ionic movement through the system and thus a reduced dormant period and a more intense acceleration peak. It has also been found in a companion study that the potassium silicate activator is about 3 to 5 times less viscous than the sodium silicate activator of the same M_s (Vance et al., n.d.). This also contributes to faster ionic movement and consequently increased early age reactivity in the K-silicate activated slag pastes. Figure 10(c) shows the cumulative heat flow curves for the Na- and K-silicate activated pastes proportioned using two different activator M_s values. The K-silicate activated pastes demonstrate higher cumulative heat flow at the end of 72 h of test as compared to the Na-based binders for the same activator M_s for reasons described earlier. The larger dormant period in the activated slag systems, especially for the Na-silicate activated ones, results in a plateau region in the cumulative heat curves (Chithiraputhiran and Neithalath, 2013; Ravikumar and Neithalath, 2012b).

4.1.2 Influence of external addition of hydroxide

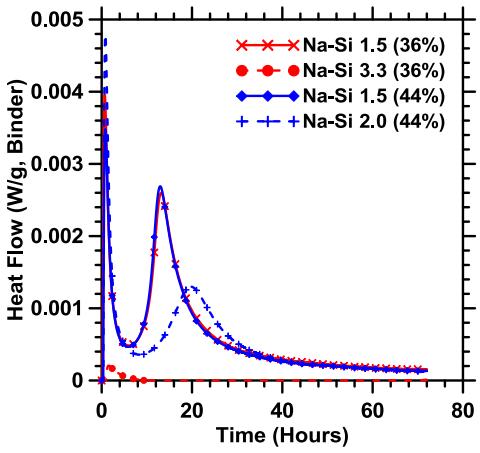

Figure 11: Comparison of heat release response of slag pastes activated using Na-silicates of different solids content and M_s.

Figure 11 shows the influences of the solids content in the Na-silicate solution and that of reducing the activator M_s through the addition of external NaOH on the heat release response of the activated pastes. The solution with a solids content of 36% had an M_s of 3.3 and the one with a solid's content of 44% had an M_s of 2.0. The amount of NaOH to be externally added is lower for the solution with a solids content of 44% (M_s = 2.0) than for the one with solids content of 36% (M_s = 3.3) to bring both the solutions to an M_s of 1.5. The magnitude of the heat release peak (and hence the extent of reaction) more than doubles when the M_s is reduced from 2.0 to 1.5, indicating the influence of relative amounts of alkali and silica in solution that results in desirable rates and amounts of reaction product formation and thus property development. The net amount of Na_2O in the system is the same irrespective of the solids content of the starting solution which makes the initial solids content in the solution irrelevant with respect to the heat release response as observed from Figure 11. For the pastes activated with the solution having an M_s of 2.0, the acceleration peak of a much lower magnitude appears after a longer

dormant period as compared to the systems made using an activator of M_s = 1.5. There is virtually no heat released when slag is activated using a Na-silicate solution of M_s = 3.3. This is attributed to an excess of silicates and scarcity of alkalis in the system at an M_s of 3.3 which prevents the polycondensation reaction as alkalis are required to sever the silica ions in silicate chains and incorporate the aluminum ion in the gel structure to form the C-(A)-S-H gel in the presence of M^+ ion (Fernández-Jiménez et al., 2003; Hong and Glasser, 2002).

4.2 Compressive Strength Development of slag mortars

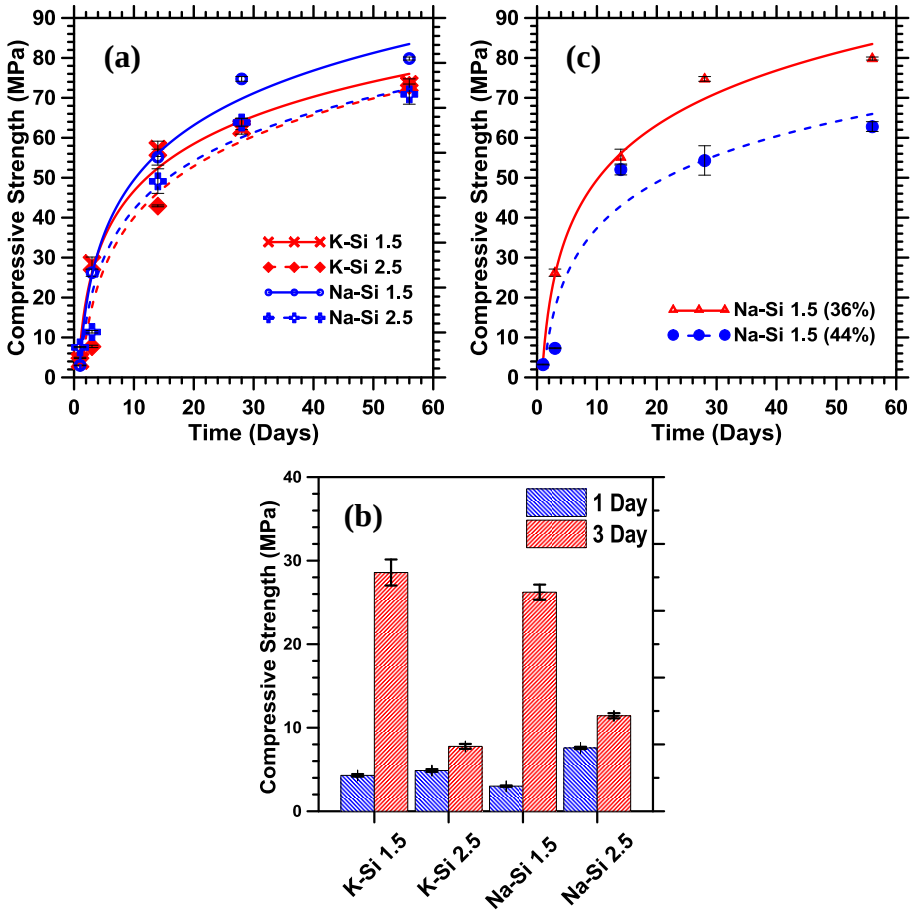

Figure 12: (a) Compressive strength development of Na- and K-silicate (36% solids content) activated slag mortars, (b) compressive strength at early ages (1 and 3 days), and (c) compressive strength development of Na silicate activated slag mortars as a function of the solids content in the Na silicate solution.

The compressive strengths of Na- and K-silicate activated mortars were determined after 1, 3, 14, 28 and 56 days of moist curing (Figure 12(a)) to understand the cationic influence on the mechanical properties of the binder. The rate of strength development provides an indication of the formation of the C-(A)-S-H gel over time in these systems. In general, it can be noticed that, at later ages (28 days and beyond), the Na-silicate activated mortar proportioned using a lower M_s (1.5) is stronger than the corresponding K-silicate activated mortar. This could be attributed to the increased amounts of reaction product formation in Na-silicate activated systems (quantified in the later section) and the likely enhancement in the degrees of silicate polymerization attributable to the Na^+ cation being able to better coagulate with monomeric silicates species (Provis and van Deventer, 2007; Ravikumar and Neithalath, 2012a). There is however no distinguishable strength difference between the Na- and K-silicate activated mortars when an activator M_s of 2.5 is used. Thus the cationic effect on mechanical properties is more evident when the cationic concentrations are higher, i.e., at lower molar M_s values of the activator. At higher activator M_s values, the silica content dominates the strength response, and the variations in the reaction product as a result of incorporation of either Na or K is expected to be minimal.

Figure 12(b) depicts the 1- and 3-day strengths of the Na- and K-silicate activated slag mortars. The higher early age strengths observed for K-silicate activated systems, especially at lower M_s can also be ascribed to the explanations provided for the heat evolution rates described earlier. With an increase in the alkali ion availability (such as for a lower M_s), the effect of increased amounts of silica in solution when K-silicates are used, is magnified. Hence the strength of the K-silicate activated mortar is higher at 1 and

3 days than the Na-silicate activated mortar when the activator M_s is lower. Figure 12(c) depicts the compressive strength development as a function of the solids content of the as-obtained Na-silicate solution. As mentioned earlier, Na-silicate with a solids content of 36% had an as-received M_s of 3.3 and the one with a solid's content of 44% had an as-received M_s of 2.0. In this case also, NaOH was added to reduce the M_s values to 1.5 so as to ensure adequate property development (Bakharev et al., 1999; Živica, 2007). It can be observed that the strength is lower at all ages when the solids content of the activator is higher. The amount of soluble silica and Na_2O is same in both the activators, with the only difference being in the amount of NaOH and water added externally. For the sodium silicate activator with a lower solids content, a higher level of NaOH addition was required as explained in the previous section. This results in a compressive strength difference of about 20 MPa at later ages when more NaOH is added to lower the M_s of the solution containing a lower solids content. In addition to improving the dissolution of ionic species from slag and facilitating increased reaction, higher NaOH addition within limits also helps incorporate more Al in the tetrahedral structures and higher degrees of silicate polymerization (Fernández-Jiménez et al., 2003; Ravikumar and Neithalath, 2012b), which are responsible for strength increase. Thus the external addition of the alkali hydroxide plays a significant role in the degree of polymerization of the aluminosilicate gel structure and the resultant mechanical properties.

4.3 TG/DTG analysis and reaction product quantification

The thermogravimetric (TG) and differential thermogravimetric (DTG) curves of alkali activated slag pastes are shown in Figures 13 and 14. Figures 13(a) and (b) show the time-dependent evolution of the reaction products for Na- and K-silicate activated slag pastes respectively when activated using alkali silicate solutions of M_s = 1.5. The main mass loss peak in the DTG curves in the 50^{o}C-300^{o}C region can be attributed to the major reaction product, C-S-H gel. It needs to be noted that the C-S-H gel in alkali activated slags incorporates significant amounts of Al, depending on the reactive Al content of the slag. When activators of high alkalinity are used, a more crystalline C-(N)-A-S-H gel has also been reported (Ben Haha et al., 2011). It can be readily observed from these figures that the total mass loss up to about 600^{o}C, which reasonably approximates the degree of reaction of these systems, is approximately the same at 28 days irrespective of the activator type. However, at an early age (1 day), the K-silicate activated paste demonstrates a much higher degree of reaction as shown by the bound water content, which is in line with the observations from isothermal calorimetry and compressive strengths. The later-age DTG curves also show the presence of a hydrotalcite-like phase with a mass loss in the range of 300-400^{o}C. Hydrotalcite phases have been commonly observed in alkali activated slag systems (Haha et al., 2012; Lothenbach and Gruskovnjak, 2007; Puertas and Fernández-Jiménez, 2003; Wang and Scrivener, 1995) and they are found to increase with increasing reaction time.

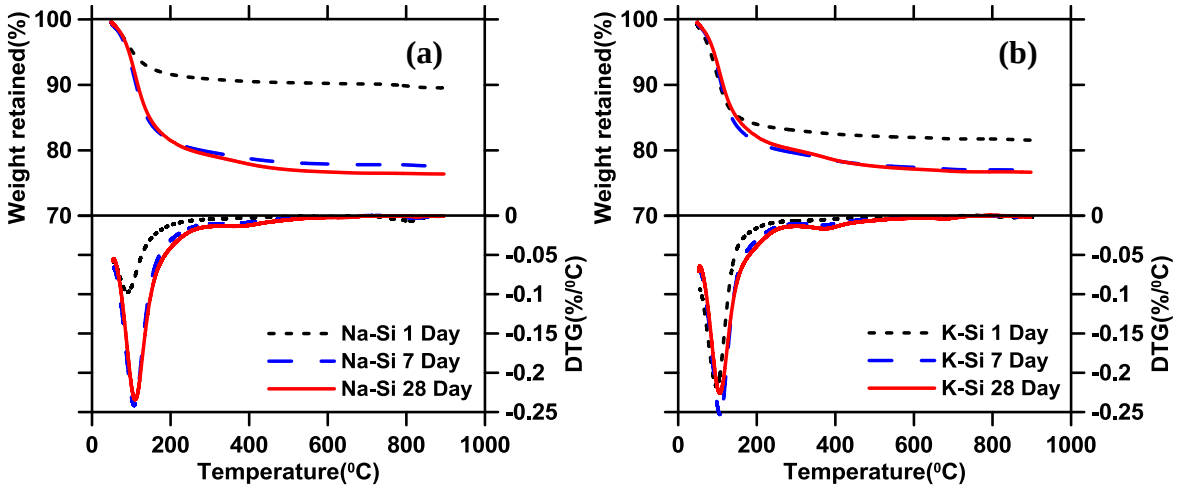

Figure 13: TG and DTG curves of: (a) Na-silicate and (b) K-silicate activated slag pastes (M_s = 1.5) after 1, 7 and 28 days of reaction.

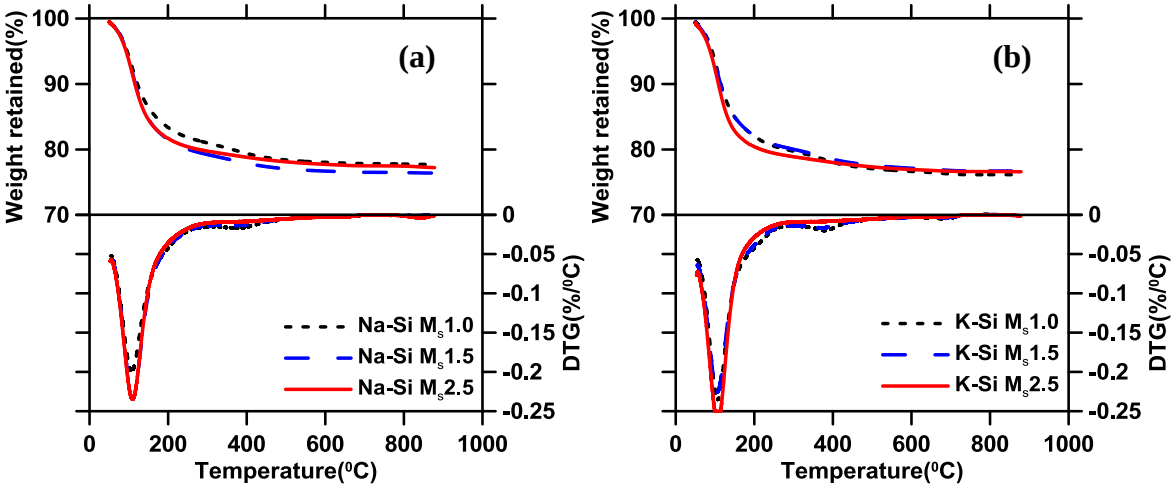

Figure 14: TG and DTG curves of: (a) Na-silicate and (b) K-silicate activated slag pastes at 28 days as a function of activator M_s

Figures 14(a) and (b) show the TG and DTG curves for 28-day hydrated slag activated using Na- and K-silicates respectively, of various M_s values. At a low M_s (or a higher alkalinity), the hydrotalcite peaks in the DTG curves are stronger for both Na- and K-silicate activation, indicating the influence of M_s on the hydration product constitution. A closer examination of the DTG plots also reveals that the hydrotalcite formation is higher for the K-silicate activated pastes, attributed to the increased basicity of the K-based

activators. When the bound water contents (mass loss up to 600^{o}C) were considered, no perceptible differences were found between the Na- and K-silicate activated pastes (of the same activator M_s) at reaction ages of 7 and 28 days.

Quantification of the amount of C-(A)-S-H gel from TG data is difficult in general because the mass loss of other reaction products like hydrotalcite overlaps with that of C-(A)-S-H in the temperature range considered. However, in this study, only a relative quantification of the reaction products is attempted. It is assumed, and rightly so, that the amount of C-(A)-S-H gel is significantly higher than the other reaction products. Also, it is assumed that the reaction product stoichiometry does not significantly change based on the type of alkali cation, M_s, or with age of reaction after 7 days. The only compositional difference that is considered here is on the Al/Si ratios of the reaction product, which were determined from ^{29}Si MAS NMR spectroscopy using the integrated intensities of resonance lines (Ben Haha et al., 2011), as detailed in the forthcoming section. For an M_s of 1.5, the Al/Si ratio was found to be 0.12, whereas it decreases to 0.10 when the M_s was increased to 2.5, irrespective of the alkali cation type. The Ca/Si ratio was fixed at 0.80 for all the pastes based on past studies (Fernández-Jiménez et al., 2013; Lothenbach and Gruskovnjak, 2007) and the H/S ratio was taken as 1.2 (Chen and Brouwers, 2007).

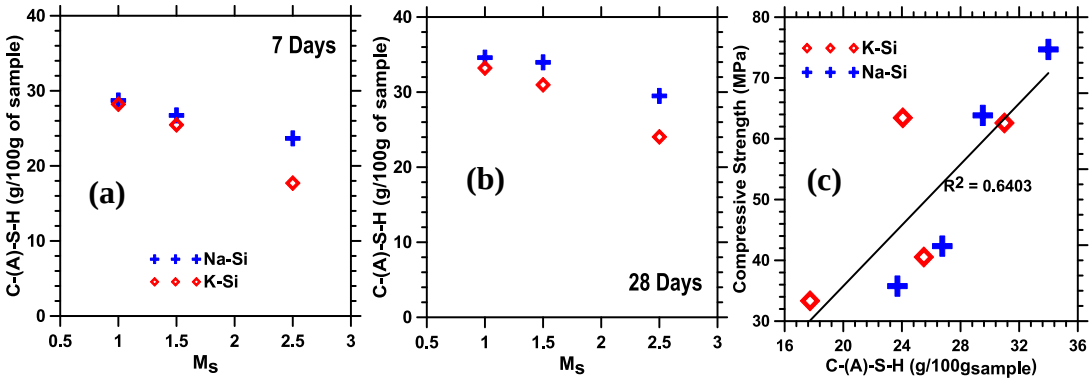

Figure 15: Amount of C-(A)-S-H (g/100g of sample) gel as a function of activator M_s for Na and K silicate activated slag pastes after: (a) 7 days, (b) 28 days of reaction; and (c) relationship between the amount of C-(A)-S-H gel and compressive strength of the mortars.

The amount of C-(A)-S-H gel formed over time as a function of the activator M_s is shown in Figure 15(a) and (b). As expected, the reaction product quantity increases with time. All the pastes show a reduction in reaction product content with increasing M_s, which is reflected in the compressive strength results also (Figure 12(a)). While the amounts of reaction products are about the same for Na- and K-silicate activated slag pastes when the M_s value is low, they are seen to diverge at higher activator M_s values, with the Na-silicate activated paste showing a higher gel content, and consequently a higher strength. This could be the result of Na^+ being strongly hydrated than the K^+ ions that influence the rate of silica dissolution, and thus the product formation at higher M_s values (Phair and Van Deventer, 2001). Notwithstanding the potential sources of errors in the quantification of the amount of reaction products, the trends mirror that of the measured mechanical properties of these systems. The NMR spectroscopic information presented in (Dakhane et al., n.d.) provides a confirmation of the accuracy of these trends, where it is shown that the amount of unreacted slag, after a reaction age of 28 days, is higher for the K-silicate activated paste for M_s values of 1.5 and 2.5. Figure 15(c) shows the relationship between the amounts of C-(A)-S-H gel and the compressive strengths. A

generally increasing strength with increasing gel content is observed; the deviations from linearity can be attributed to the differences in degrees of polymerization of the gel likely induced by the alkali cation type and the silica modulus.

4.4 FTIR Spectroscopy

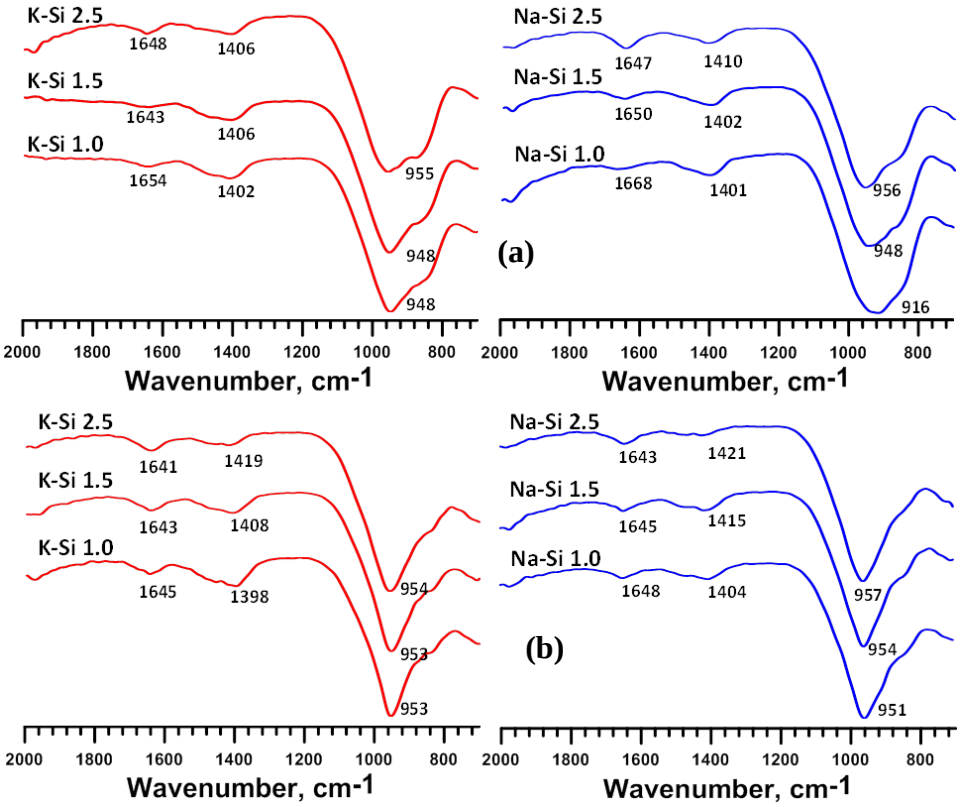

Figure 16: FTIR spectra of alkali activated slag pastes using hydroxide and silicate solutions of sodium and potassium at (a) 1 day and (b) 28 days

In Figure 16 it can be seen that the silicate peaks are consistently increasing with increase in both M_s and time. The wavenumbers corresponding to the Si-O and Al-O stretching are observed from 800-960 cm^{-1}. Also, asymmetrical stretching of C-O at around 1430 is observed. This indicates that carbonation in the one day samples for both the potassium and sodium based binders is relatively higher than that at 28 days, which is due to the

high alkalinity in the mix at early ages. The silica ion has 3 degree of polymerization depending on the no of silicon ions attached, namely Q_4, Q_3 and Q_2. There are variety of these silicate chains formed in the mix. The degree of polymerization or crystalline nature depends on the formation and densification of these structures over time.

It can be noted that the silicate peaks are higher for K-silicate as compared to the Na-silicate based binders at day one. However at 28 days, the Na-silicate peaks are consistently higher at all the M_s values. As potassium has the capacity to keep soluble silica stabilized for a longer duration, giving higher peaks for the K-silicate based binder at day one. Although when its stabilizing effect reduces over time and the sodium ion is incorporated into the gel structure, more than that by the potassium ion at 28 day. More aluminum incorporation in the silicate gel structure with Na^+ ion leads to the reduction in the wavenumber of the silicate peak at lower M_s, this explains the early age strength of K-silicate mixes being higher than the Na-silicates at same M_s. The higher wavenumber corresponds to better polymerization and the gel having a higher species of the aluminosilicate bonds.

It can also be noticed in both silicate mixes at 1 day, that the silicate peaks are not sharp and has a shoulder on the lower side. This could be due to the less polymerized silica (monomers, diamers and olignomers). Its only when Al gets incorporated to form tetrahedral chains with alkali cation substituting the silicon ion. However the shoulder is sharper and distinct in the K-silicate mixes. It is known that K^+ ion favors olignomers and thus does not form much variability thus limiting to narrow spectrum or a degree of polymerization (Q_2). On the contrary Na^+ ion shows a wide variability in the structures formed due to its capacity to favor monomer and diamer silicate chains. Thus the

shoulder on Na-silicate based mixes are much smoother and are broad as compared to K-silicate ones.

Thus in the 28th day data it is noticed that the shoulders are now converged into the main silicate peak and the peak is now much sharper. This indicates the densification of the silicate structure and the gel being in consistent degree of polymerization. Moreover peaks at higher wavenumber are observed for Na-silicate based mix with the exception at M_s 1.0.

Depending on the activator alkalinity, cation polarity and the age of the specimen, the two major reasons can be deduced that can be attributed to the increase in the wavenumber, they are: (i) modification in the C-(A)-S-H gel due to the higher degree of silicate polymerization and reduced Al incorporation, aided by the increased amount of alkalis, and/or (ii) the formation of segregated Si rich gels with Ca.

4.5 Summary

It was observed that the K-silicate activated slag pastes demonstrate higher heat of reaction after 72h. The induction period was shorter and the intensity of the acceleration peak higher for the K-silicate activated systems at lower M_s values than those activated with Na-silicate showing the effectiveness of K-based activators, including those contributed by the smaller solvated radius of K^+ and lower viscosity of the activator, in early-age reactions. The early-age compressive strength results also validate this observation. At later ages, the compressive strengths are higher for the Na-silicate activated systems at lower M_s attributable to the effects of increased amounts of Na that likely result in a more crystalline reaction product. Increasing the silica content of the activator resulted in comparable later-age strengths irrespective of the alkali cation type.

An approximate quantification of C-(A)-S-H gel utilizing the thermal analysis results along with the gel stoichiometry from published literature showed reducing amounts of reaction product with increasing M_s for both activator types beyond 7 days of reaction. At later ages, the Na-silicate activated pastes showed higher amounts of reaction product formation from TG analysis which corresponds to the trends in compressive strength.

5. EFFECT OF CATION ON REACTION KINETICS AND PRODUCT FORMATION IN SLAG BINDERS ACTIVATED USING ALKALI SILICATE POWDERS AND HYDROXIDES

The characteristics and type of the activating agent plays a significant role in determining the reaction rate and its extent, and also on the type of reaction products formed. This inherently affects the early- and later-age properties of the final binder system (Hajimohammadi et al., 2011; Puertas et al., 2004; Wang et al., 1994). Alkali silicate solutions with different silicate modulus (M_s) have been extensively studied for their effectiveness in producing strong and durable binders under standard moist curing conditions, specifically for source materials containing reactive calcium (e.g. slag). There were three cases made by varying changes in the two parameters 'n' and the 'M_s'. The three cases are as follows:

1. Constant 'n' of 0.05 with 'M_s' varying between 1.0, 1.5 and 2.0.
2. Constant 'M_s' of 1.5 with 'n' varying between 0.02, 0.03 and 0.05.
3. Constant 'M_s' of 2.0 with 'n' varying between 0.03, 0.05 and 0.07.

The results of all the experiments are provided in accordance with the three cases as explained above. The aim was to understand the influence of cation when one of the activator concentration or the silica modulus was altered by keeping the other parameter constant. The powder silicates added to the activators were insoluble in certain cases and this had an influence over the reaction product formation over time. In this chapter the activator characteristics, the mechanical properties of slag activated with sodium and potassium silicate powders and hydroxides are explored. Isothermal calorimetry is used

to understand the effect of the activator characteristics, along with distinguishing the fundamental differences in early age reaction kinetics when powdered form of sodium silicate and potassium silicate activators are utilized. The fundamental differences between the two types of powder activators mostly relate to the dissolution effects of the powder and are brought out through the use of TGA and FTIR spectroscopy.

5.1 Activator characteristics of powder activators

Solubility of the hydroxide and the silicate powders in water is a key factor in the reaction kinetics of the slag pastes. It was observed that the potassium silicate powders were soluble with the potassium hydroxide and a homogeneous activator solution was obtained at the M_s of 1.0, 1.5 and 2.0. This allowed for very consistent results varying with M_s for the potassium silicate based mixes.

However for the sodium silicate powder mixes, the activators with a lower M_s of 1.0, there was a precipitation of the sodium silicate powder. This was caused due to more sodium hydroxide in the solution which dissolved better and due to its dissolution in water; there was less space available for the silicate powder. However at higher M_s of 2.0 with less hydroxide available compared to the silicate, there was a homogeneous solution obtained with no precipitation of the silicate powder. This could be attributed to the size of the hydration spheres of the sodium and potassium ion (Fernández-Jiménez et al., 2013). Due to the higher charge density of the sodium ion, there is more affinity for water to attach itself to the ion and thus forming a larger hydration sphere which occupies more space in the solution matrix. This allows less space for the silicate ions for dissolution causing it to precipitate at lower M_s. On the contrary the potassium ion has a less charge

density which in turn forms a smaller hydration sphere and occupies less space thus allowing for a homogeneous dissolution for the silicate in the solution as well.

5.2 Isothermal Calorimery of slag pastes

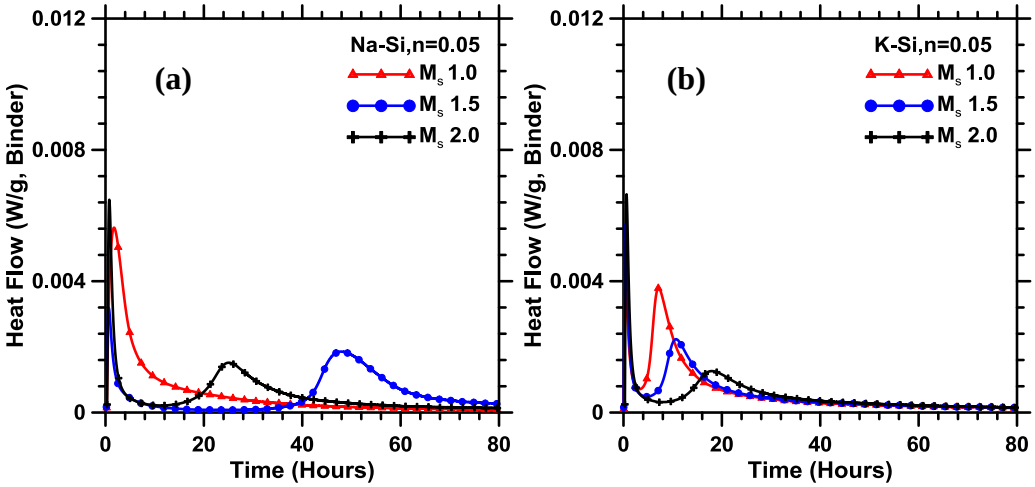

Figure 17: Isothermal calorimetry of slag activated with (a) sodium silicate and (b) potassium silicate powders with n = 0.05 and M_s of 1.0 to 2.0

Figure 17(a) and (b) shows the heat evolution curves of slag using an n value of 0.05 and M_s values of 1, 1.5 and 2. The experiments were carried out at 25°C. The calorimetric response exhibits two main peaks. The very narrow peak that occurs within the first two hours of mixing generally corresponds to the particle wetting and the dissolution of the slag particles (Ravikumar and Neithalath, 2012b; Shi and Day, 1995). However, in these particular mixes, the dissolution peaks are most likely not accurate as isothermal conditions are not reached, although they give a comparative idea between the mixes. The induction period of the these samples is considerably longer than that of OPC pastes, in line with the observations reported previously (Chithiraputhiran and Neithalath, 2013; Ravikumar and Neithalath, 2012b). This is due to the time required for the ionic species in solution to reach a critical concentration before depositing reaction products on the

particle surfaces. The sodium silicate with M_s 1.0 shows just one initial peak which is associated with hydroxide activated pastes; this can be attributed to the activator characteristics explained earlier. However for M_s 1.5, a longer dormant period is observed which shows that it takes longer for silicates to reach critical concentration. For M_s 2.0 a shorter dormant period followed by a lower acceleration peak is observed. More silicates in the mix give a lower acceleration peak as there are not enough hydroxide ions to enhance the reactivity. For the potassium silicate mixes, activator solution was homogeneous which allowed for consistent results. With a decrease in M_s (increase in alkalinity) there was a shorter dormant period followed by a higher acceleration peak, which hints at higher reactivity. This is also due to the reactivity of K^+ hydrated ions being comparatively more reactive than the Na^+ hydrated ions. Thus at the same n of 0.05, the potassium silicate mixes give a much faster and higher acceleration peaks as compared to that of the sodium silicate mixes. Studies have found that when alkaline activation is insufficient and becomes the main factor slowing down the hydration of slag, a lower silica modulus is preferred, with the optimum moduli for basic slag lying between 1.0-1.5 (Wang et al., 1994). Also at high M_s ratios, there are not enough OH^- ions present in solution to adequately stabilize the solution and polymerization proceeds fairly quickly leading to high viscosity values with dissolutions rates also expected to be lower. A lower M_s ratio is expected to increase nucleation and crystal growth, which will provide for the expulsion of water from the newly formed structure leading to an initial decrease in viscosity. However if the M_s ratio is too low, the increased solid content of the paste starts to become a destabilizing factor while most added Na or K ions cannot be accommodated in the final structure (van Jaarsveld and van Deventer, 1999).

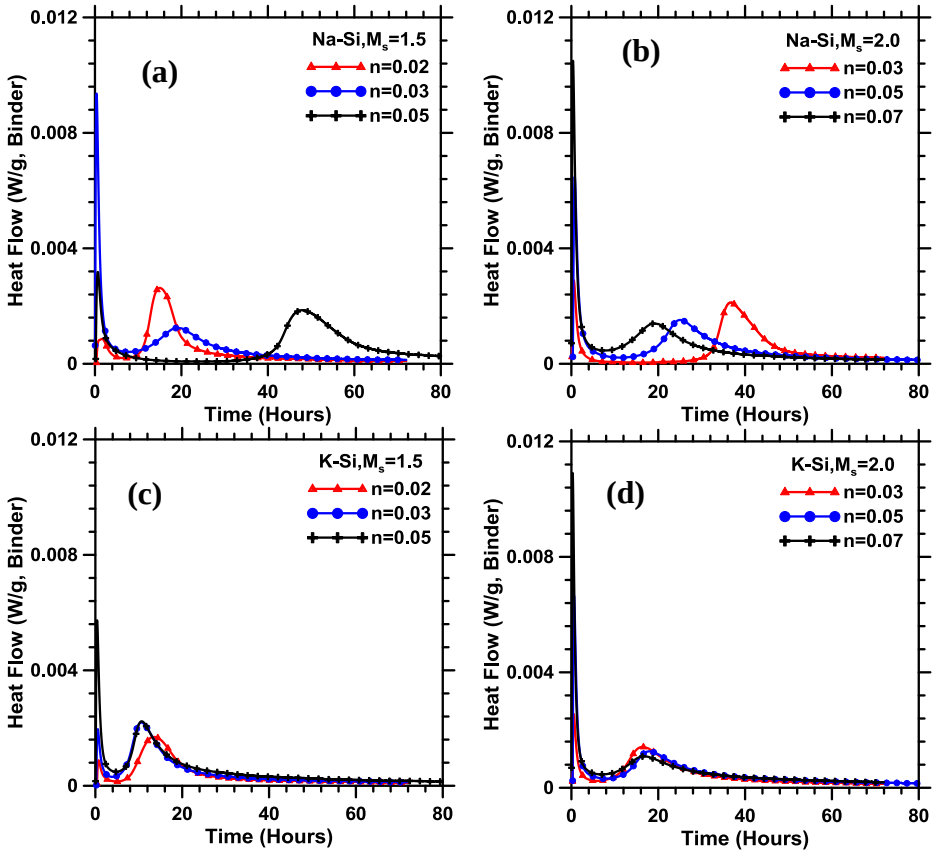

Figure 18: Heat evolution of slag activated with sodium silicate with an M_s of (a) 1.5 and (b) 2.0 and potassium silicate with an M_s of (c) 1.5 and (d) 2.0.

Figure 18 (a) and (b) above shows the calorimetric heat plots indicate that the initial dissolution peak is a function of the activator concentration (n) and the acceleration peak is a function of the M_s. With the increase in 'n' the alkalinity of the mix increases but the M_s being the same allows for a proportional silicate content. Thus for the potassium based mixes, the acceleration peak is superimposing each other at all the 'n' values. However the initial dissolution peak increases with n. This shows that even when the dissolution is more, neither the induction phase nor the acceleration phase is altered in case of the potassium silicate mixes. However in Figure 18(a) and (b) the sodium silicate mixes show that at M_s of 1.5, with a lower n, the induction phase is shorter and thus

indicate that with more ‘n’ it takes longer to reach a critical concentration to start the acceleration phase. At ‘n’ of 0.02 there are not enough hydroxide ions to precipitate the silicates and hence an acceleration peak occurs early on. At ‘n’ of 0.03 there are enough hydroxides and do not allow the silicates to dissolve which leads to an acceleration peak but is not higher than that of ‘n’ of 0.02. Thus at ‘n’ of 0.05 the induction period is longer as the silicates are not dissolved well in the activator media due to their high concentration. Also the acceleration peak intensity is also less than ‘n’ of 0.02. This is reflected in the early age compressive strength results.

When the M_s is kept at 2.0 and the ‘n’ is varied from 0.03, 0.05 and 0.07 as shown in Figure 18 (b). With more silicates proportional to the hydroxide, there is less hydroxide to displace the silicates out of the solution to precipitate out. Thus with more homogeneous silicates in the activator solution media, the results are consistent and with a higher ‘n’ the induction period is shorter and the acceleration peak intensity is smaller. The solubility of the silicates and the hydroxides, thus affects the activator characteristics which in turn affects the dissolution and acceleration phases of the heat flow curves.

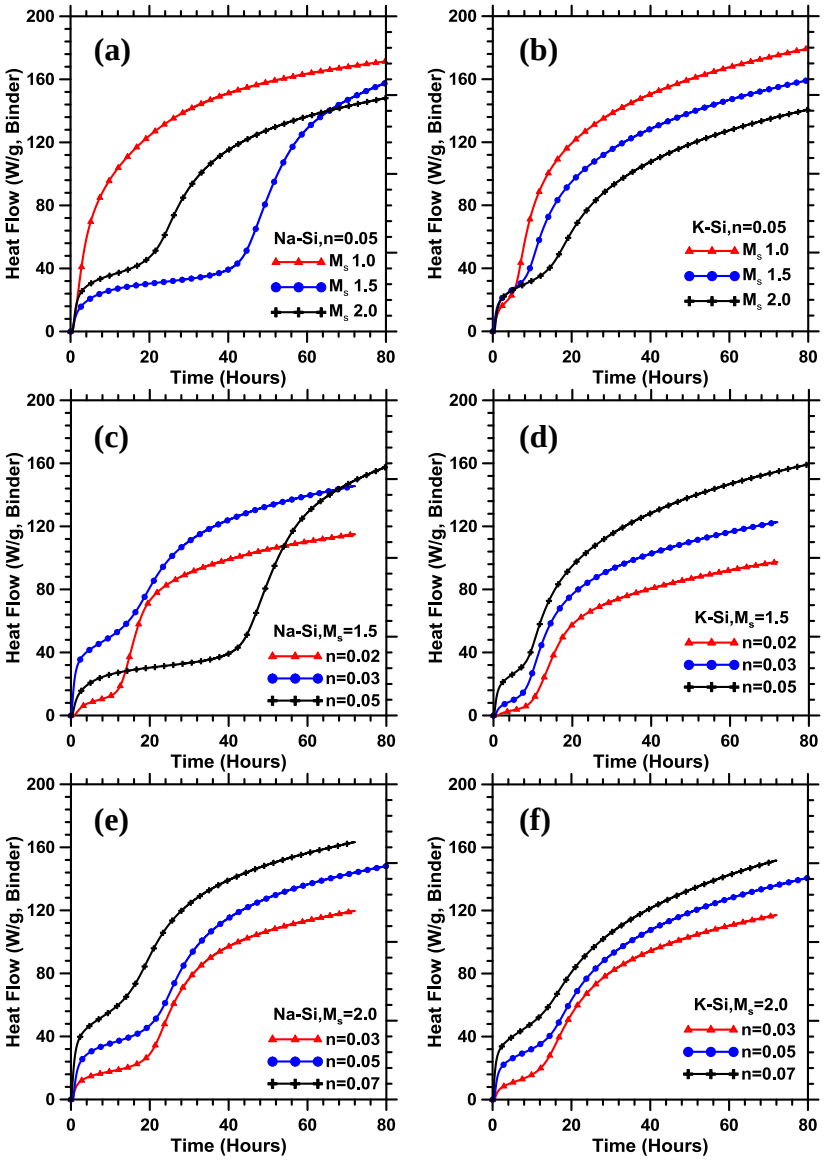

Figure 19: Cumulative heat release response for slag activated with a constant n of 0.05 of (a) sodium silicate, (b) potassium silicate, (c) sodium silicate and (d) potassium silicate with constant M_s of 1.5. (e) sodium silicate and (f) potassium silicate with a constant M_s of 2.0.

Figure 19 shows the cumulative heat plots of the different mixes and the potassium silicate mixes show consistent results. However the sodium silicate mixes show non consistent trends that is explained in the previous section. The curves however at the end of 72 hours asymptote to values that are consistent which are then in order of increasing

or decreasing ‘n’ or the M_s. In Figure 19(a) lower M_s at the end gives the highest heat and then the M_s of 1.5 followed by M_s 2.0. Figure 19(c) shows that at the end of the test the ‘n’ of 0.05 has the highest heat followed by ‘n’ of 0.03 and 0.02. Thus the total energy in the system is increasing consistently with a decrease in M_s and an increase in ‘n’ in both sodium and potassium silicate systems.

5.3 Compressive Strength Development on Slag Mortars

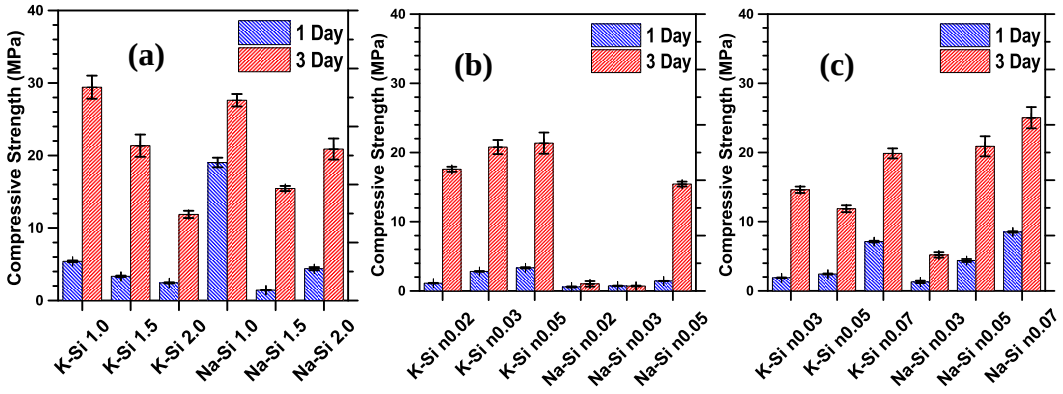

Figure 20: Heat evolution of slag of (a) with constant ‘n’ of 0.05,(b) with a constant M_s 1.5 and (c) M_s of 2.0

The early age strengths conform to the calorimetric results. Figure 20(a) shows that the potassium silicate based mixes have an increase in strength with decrease in M_s. However the sodium silicate based mixes show a high early strength for M_s of 1.0 followed by M_s of 2.0 then by M_s of 1.5, which is caused due to the insolubility of the silicates at lower M_s where the high hydroxide content does the work of dissociation giving an enhanced reactivity. The trends followed at 1 day are also followed at 3 days proportionally. Figure 20(b) shows that the sodium based system shows no strength gain at low ‘n’ which is due to less reactivity and dissociation. However at ‘n’ of 0.05, there a drastic strength gain at 3 days, which indicates the silicates reacting in the mix. Being in powdered form and insoluble during the mixing phase they react locally when the paste has hardened. On the

contrary the potassium silicate based mixes show a uniform strength gain with an increase in 'n'. The trends followed for 1 day are repeated proportionately for the 3 days as well with the exception of sodium silicate with an 'n' of 0.05. Figure 20(c) shows that the sodium silicate based mixes show a regular trend in strength gain with an increase in 'n' at a higher M_s. It could be due to less hydroxide in the system to displace the silicates from the mix as explained earlier in the calorimetry. The potassium silicate strengths also increase with increase in 'n' for 1 day strengths but show a slight decrease for the 'n' of 0.05 at 3 days which could be due to silicates not completely dissolved.

The early age strengths can be affirmed and explained by the isothermal calorimetry results. The solubility of both sodium and potassium silicate powders in a system with hydroxide defines the early age mechanical strength gain attributable to the reaction kinetics of the system. However these trends are not followed at the later age and are shown below.

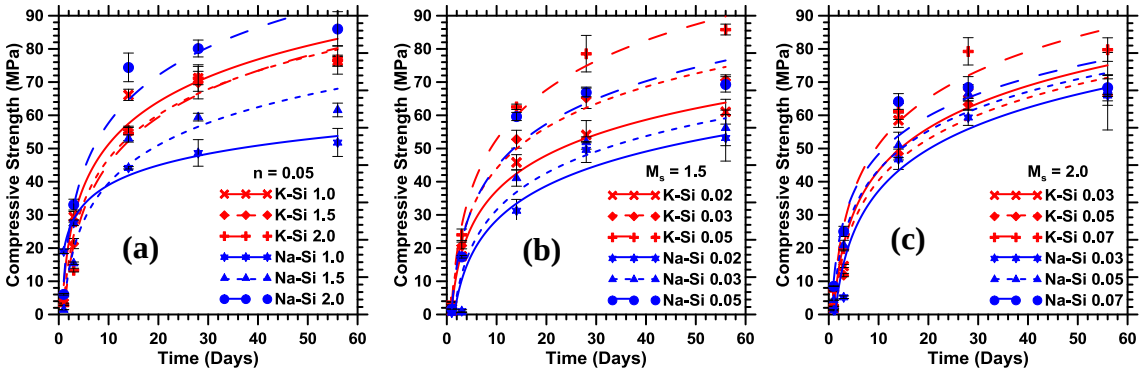

Figure 21**:** Compressive strength of 56 days slag mortars at (a) 'n' of 0.05 (b) M_s of 1.5 and (c) M_s of 2.0.

Figure 21(a) shows that the sodium silicate based mixes have a huge impact of solubility of silicates on the strength. The sodium silicates on the other hand shows a strength of 50

MPa for M_s of 1.0 and then the strength increases with increase in M_s and rises up to 85 MPa for M_s of 2.0. However potassium silicate based mixes asymptote to same strength at a given 'n' of 0.05. This indicates that there is no influence of hydroxide on potassium silicates at later age. Figure 21(b) indicates a significant difference in the strengths at later ages, with an increase in 'n' at an M_s of 1.5. The potassium silicate based mixes perform consistently higher than the sodium silicate ones. Also the strength increase with an increase in 'n' is much more for the potassium silicates mixes than for the sodium silicate mixes. It is due to more dissociated species available to polymerize at later ages, which explains the higher strength for a higher 'n'. At a lower M_s there is more hydroxide in the activating media thus allowing for a better dissolution allowing for magnified differenced in the strength gain. Figure 21(c) at an M_s of 2.0, the difference in the 'n' is reduced and the trends are converged as compared to that given in Figure 21(b). The sodium silicate mixes show all asymptote to similar strength at the end of 56 days at approximately 68 Mpa. However the strength gain at 28 days indicates that the strength increased with an increase in 'n'. For the potassium silicate mixes the 'n' of 0.07 shows the highest strength and has converged at 28 days at around 80 MPa. The 'n' of 0.02 and 0.03 asymptote to similar values with the sodium silicate mixes. Thus the effect of cation is reduced at low 'n' values at a higher M_s. It can be concluded that with a higher M_s the influence of the cation is reduced which is a similar trend that was observed in Chapter 4 with liquid silicate activators. The influence of cation is thus profound at lower M_s due to more hydroxide addition.

5.4 TG/DTG analysis and reaction product quantification

TG/DTG analysis indicated that the loss associated with water was the highest for the 1 day pastes. It can be seen in Figure 22 that the peak associated with water is deeper for the sodium silicate mixes as compared to the potassium based mixes, which indicates more bound and free water is present in the hydrated reaction product of sodium silicate mixes. In Figure 22(c), (d), (e) and (f) it can also be noticed that the peaks are sharper for the M_s of 1.5 than for the M_s of 2.0. When the peak is sharper there is more free water in the system than bound water, this can be attributed to the fact that bound water evaporates at a temperature above 100^0C. More bound water is related to more reaction product i.e. calcium alumino silicate hydrate (C-(A)-S-H), being formed in the mix. This conforms to the early age compressive strength results obtained in the previous section.

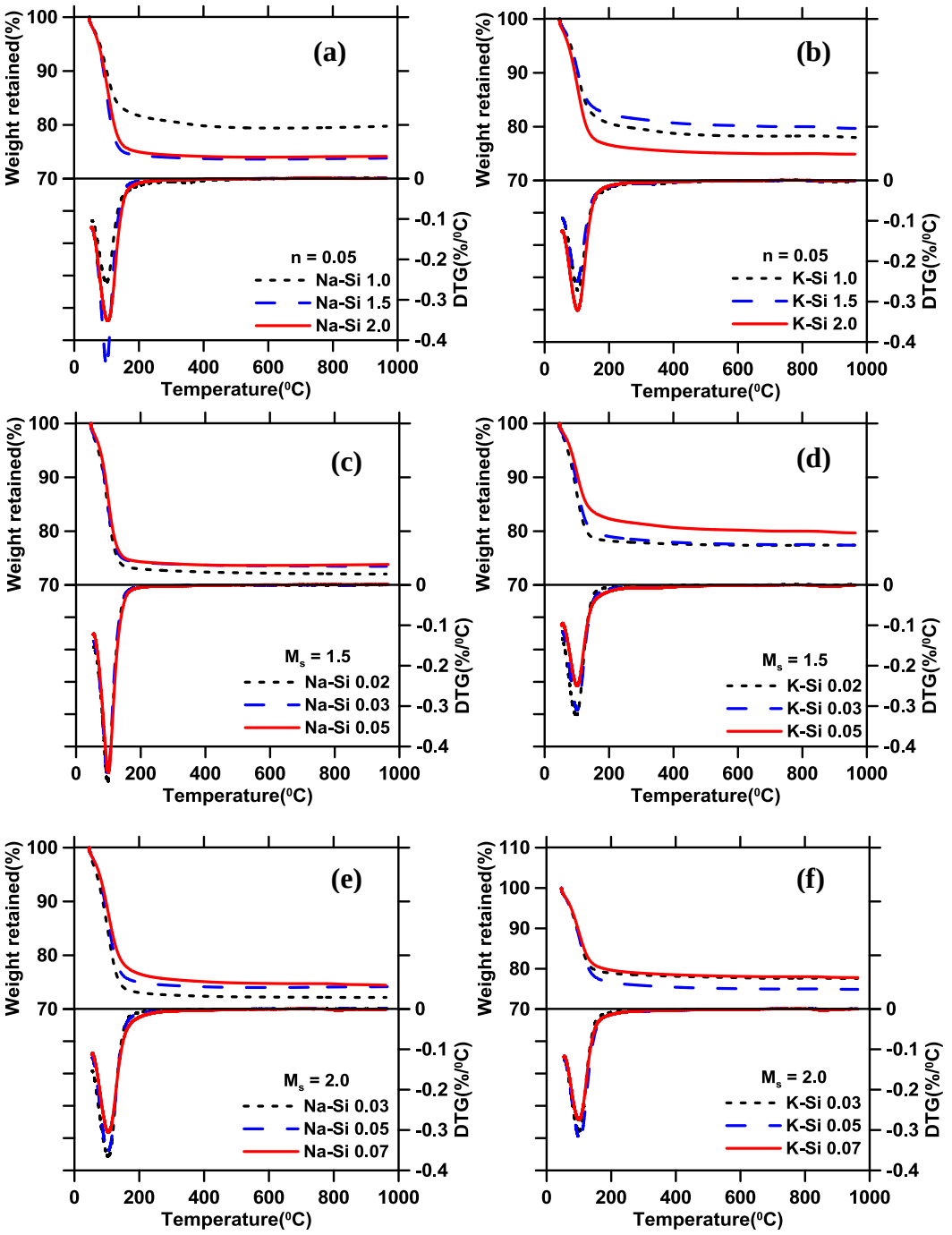

Figure 22: TG/DTG curves for 1 day pastes with 'n' of 0.05 for (a) sodium and (b) potassium, with M_s of 1.5 for (c) sodium and (d) potassium and with M_s of 2.0 for (e) sodium and (f) potassium based mixes

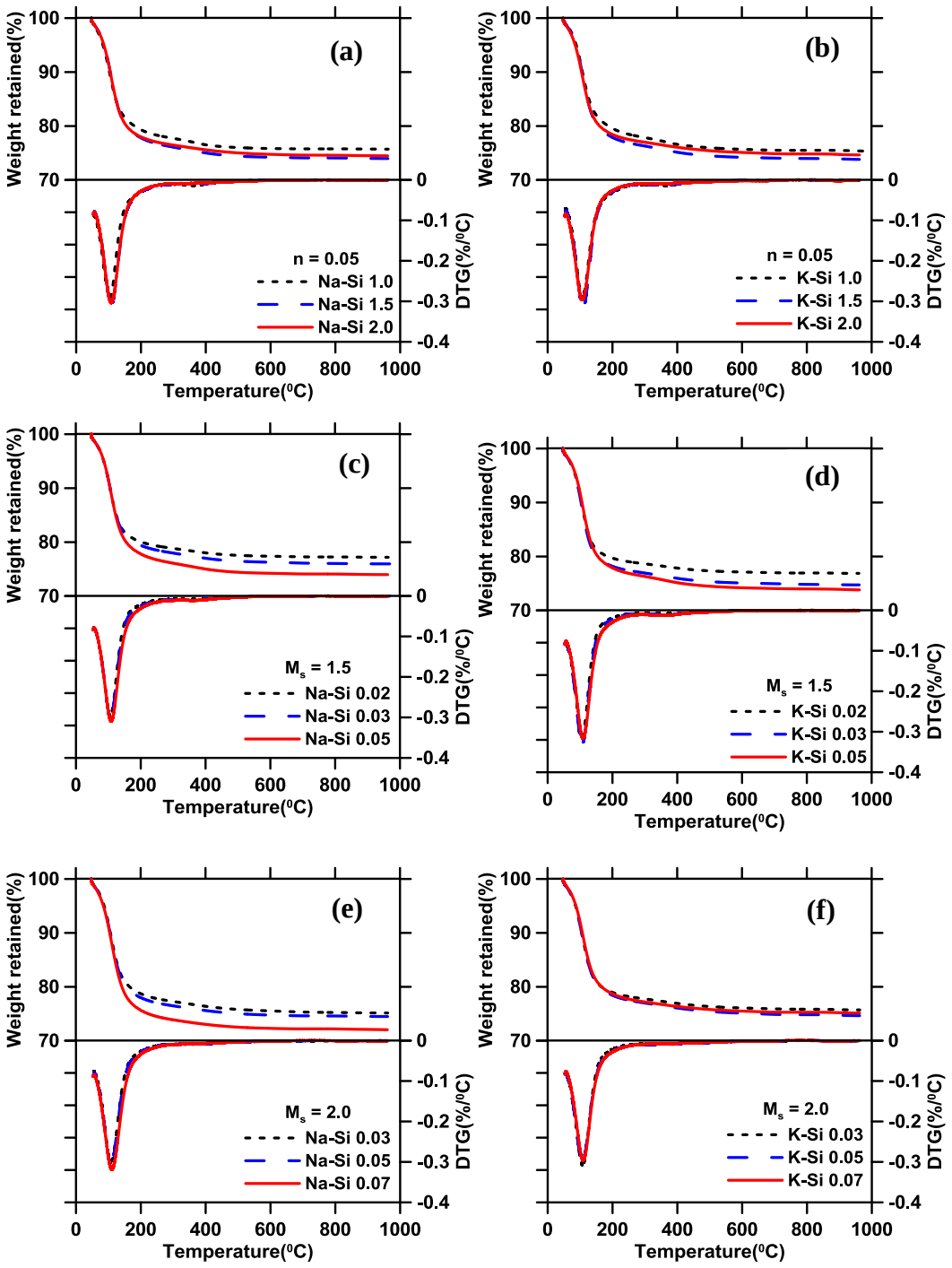

Figure 23: TG/DTG curves for 7 day pastes with 'n' of 0.05 for (a) sodium and (b) potassium, with M_s of 1.5 for (c) sodium and (d) potassium and with M_s of 2.0 for (e) sodium and (f) potassium based mixes

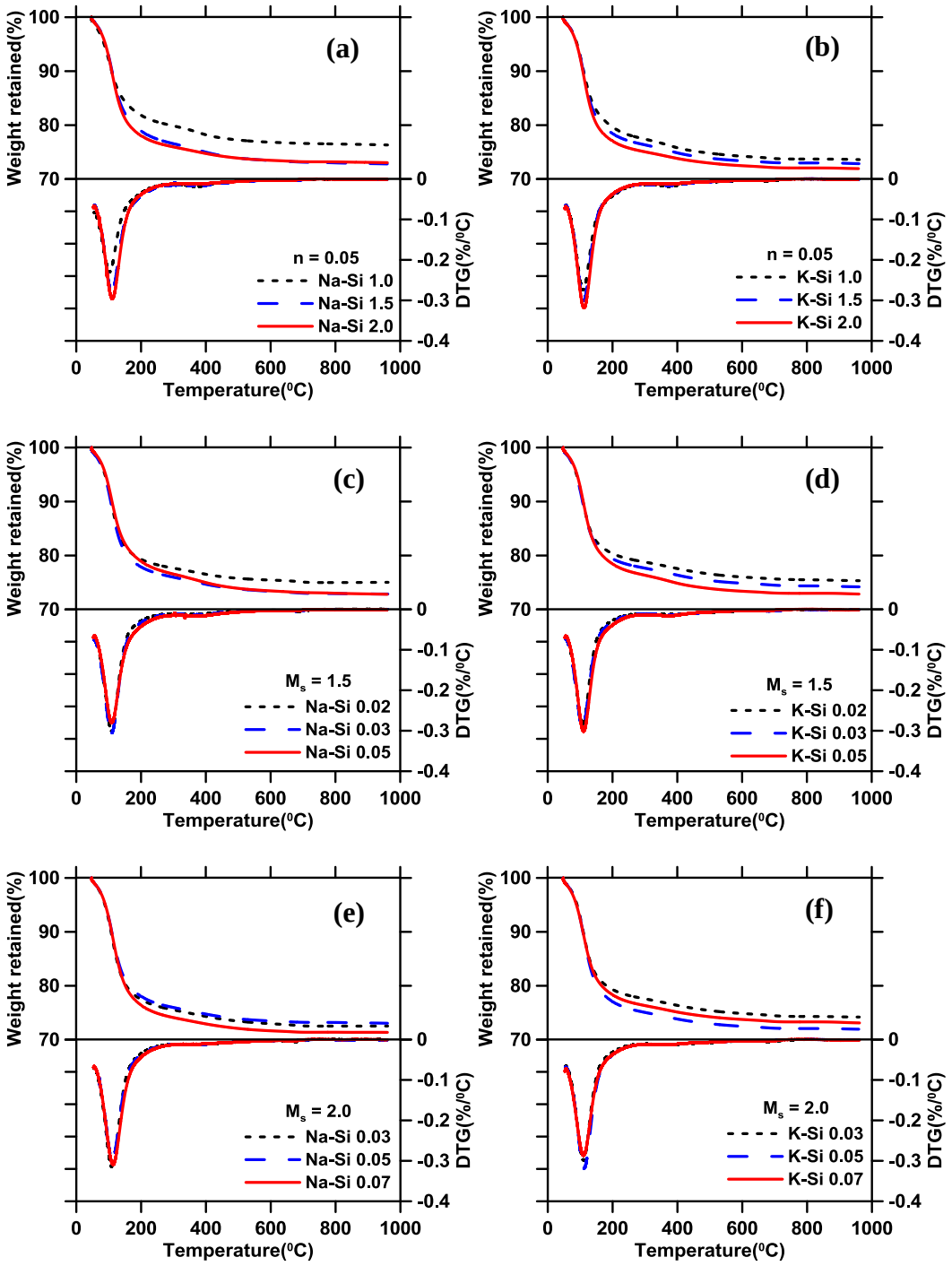

Figure 24: TG/DTG curves for 28 day pastes with 'n' of 0.05 for (a) sodium and (b) potassium, with M_s of 1.5 for (c) sodium and (d) potassium and with M_s of 2.0 for (e) sodium and (f) potassium based mixes

Figure 24 shows that depth of the peaks reduced with time and is noticed at 28 days. Hydrotalcite peaks are significant at 400^0C. The water associated with the reaction product lies between 150^0C to 300^0C, thus the mass lost can be associated with the reaction product for its quantification. The quantification of the C-(A)-S-H gel can be done using the stoichiometric values. The gel quantified is shown in Figure 24.

Figure 24 (a) indicates that the reaction product is formed more for the potassium silicate at 1 day with a decreasing M_s. This trend stays consistent at 7 and 28 days with increase in the gel formation. However for sodium silicate mixes, the gel formation is the least for M_s of 1.5 at 1 day but is the highest at 7 and 28 day. It can be attributed to the less solubility of the silicates due to the hydroxide content initially, however due to the dissociation caused by the hydroxide; there were species from slag to react with. Figure 24(b) and (c) show that with an increase in 'n' there was more reaction product. It is also seen that the reaction product formed at 28 days is more for the sodium silicate mixes as compared to that of the potassium silicate mixes. However formation of more reaction product cannot be entirely attributed to the high compressive strength. In the next section the degree of polymerization is discussed, which shows that potassium silicate mixes reach a higher degree of polymerization and thus the potassium silicate mixes, show a higher strength despite having less reaction product formation. Figure 25 below shows the reaction product growth over 1, 7 and 28 days with constant n and M_s.

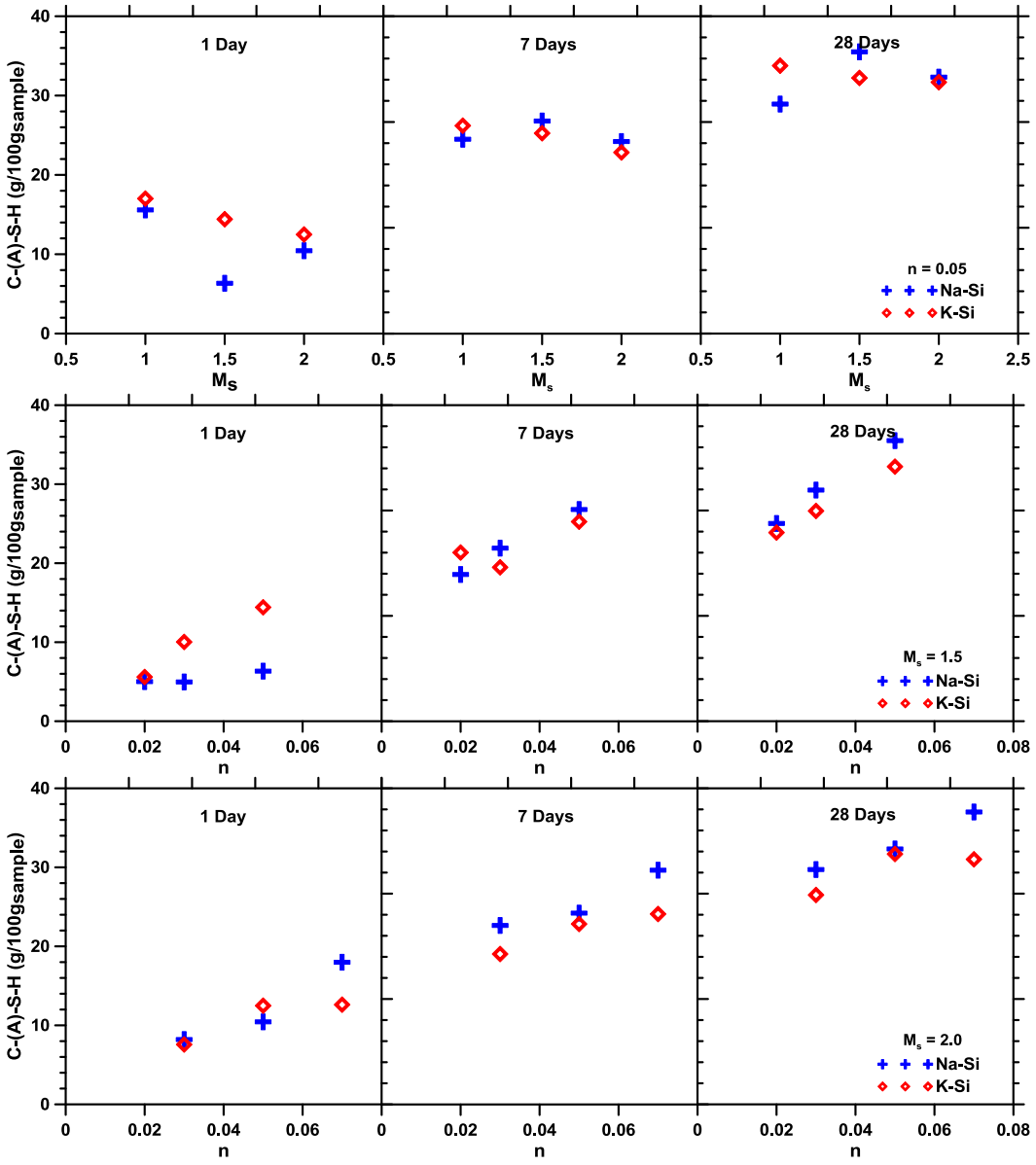

Figure 25: Amount of C-(A)-S-H (g/100g of sample) gel as a function of M_s with a constant 'n' of (a) 0.05 and activator 'n' at constant M_s of (b) 1.5 and (c) 2.0 for Na and K silicate activated slag pastes at 1, 7 and 28 days

5.5 FTIR Spectroscopy

It has been established that the alkali activation of slag results in the formation of a low Ca/Si ratio C-S-H and C-A-S-H gels as the principal reaction product (Song et al., 2000; Wang and Scrivener, 1995, p. 199; Yip et al., 2005). The discussions in this section will be limited to the stretching vibrations of Si-O-Si units, as they can be used to represent the signature of the composition of the reaction products. In general the Si-O-Si stretching bands are observed at a wavenumber of 950-1000cm^{-1} (Bernal et al., 2011; Garcia-Lodeiro et al., 2013). Figure 26 shows the FTIR spectra of the starting slag showing one main peak occurring at 928 cm^{-1} recognized as the Si-O stretching of the SiO_4 tetrahedral (Fernandez-Jimenez et al., 2007). In the alkali activated slag pastes, this band representing the asymmetric stretching vibrations of the Si-O-Si bands has been shifted to higher wavenumber values of 940-955 cm^{-1}. Figure 27 represents the 1, 7 and 28 day FTIR spectra of the potassium silicate and sodium silicate activated slag pastes. The observed shifts of the Si-O-Si stretching bands can be attributed to the formation of a more condensed tetrahedral species (Chithiraputhiran, 2012). The FTIR spectra also contains bands of calcite (C-O) occurring at 1370-1420 cm^{-1} that occurs in the event of carbonation. The peaks detected between 3330-3375 cm^{-1} and 1630-1645 cm^{-1} represent stretching and bending modes of OH^- groups present in H_2O and the hydration products. The distinct peaks of calcium hydroxide (CH) that occur at ~3365 cm^{-1} in most OPC pastes is absent in the spectra of slag as CH cannot precipitate in these systems due to its higher solubility compared to C-S-H and C-A-S-H (Chithiraputhiran, 2012).

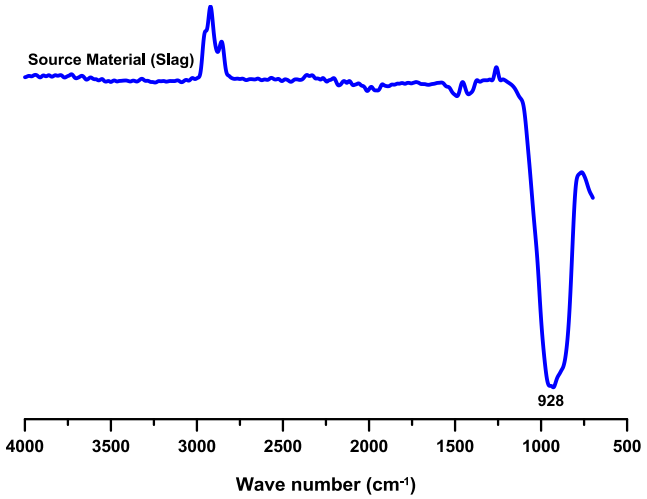

Figure 26: ATR-FTIR spectroscopy of slag

A shift to a higher wavenumber generally indicates the effect of a high Si content within the C-S-H gel (or a lower Ca/Si ratio) (Palacios and Puertas, 2006). Thus, it is expected that the pastes activated using higher M_s values (in which case the content of SiO_2 is increased) shows characteristic signatures shifting towards higher wavenumbers, as shown in Figure 27. This trend is more pronounced with longer curing durations. The solubility of Si is known to increase with pH content of the paste, whereas that of Ca decreases. Hence, the systems activated with high silica concentrations, i.e. higher M_s values, tend to produce C-S-H gels with a lower Ca/Si ratio. This results in the production of a Q^3 silicon that has the ability to cross-link between adjacent silicon chains (Fernandez-Jiménez et al., 2006). This is in contrast with the C-S-H gels produced in OPC pastes which predominantly contain Q^1 and Q^2 units (Schneider et al., 2001). The IR absorption bands witnessed in the range of 920-960 cm^{-1} in Figure 27,28 and 29 are consistent with the predominance of Q^2 and Q^3 silicates (Dimas et al., 2009).

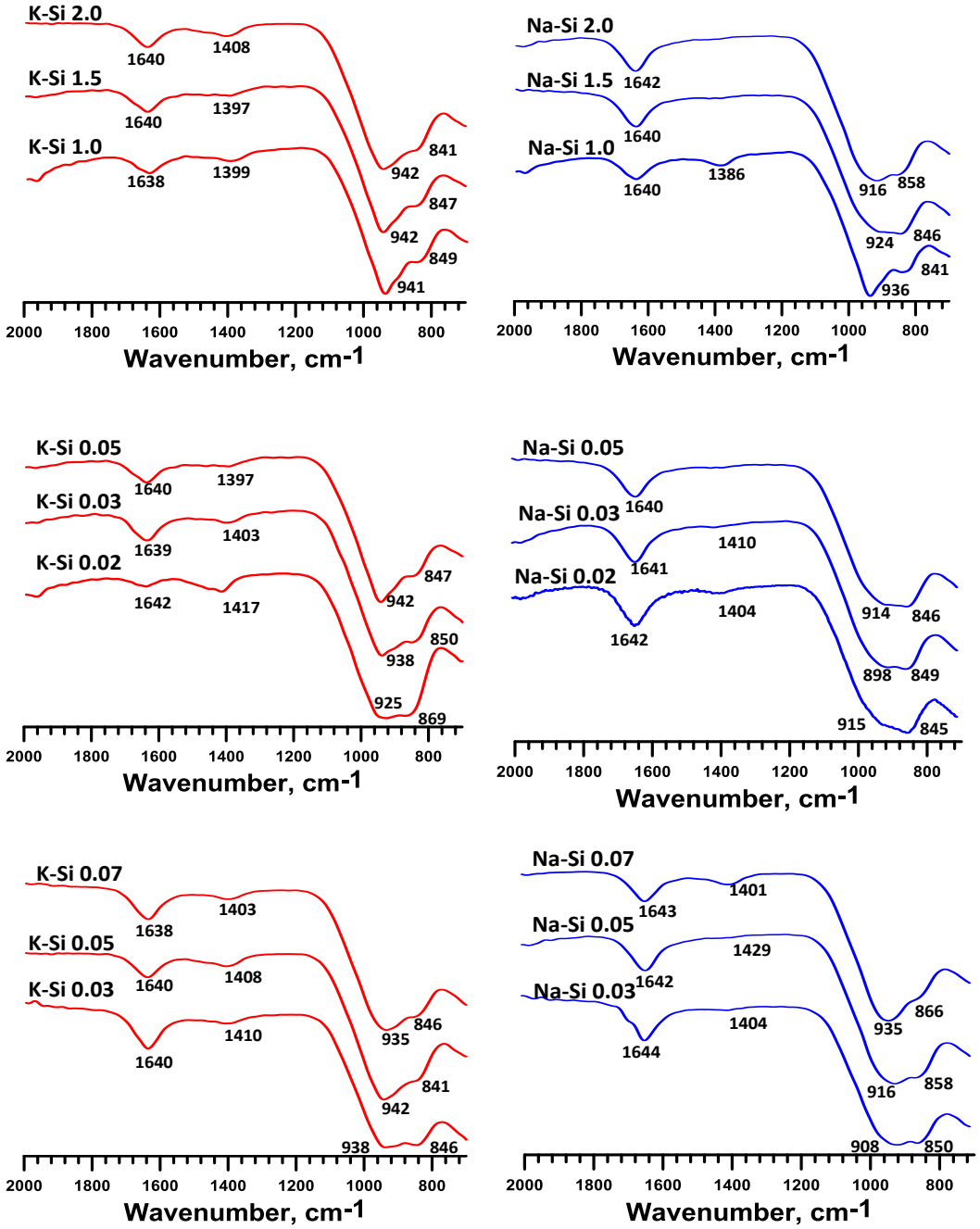

Figure 27: FTIR spectra for 1 day pastes with 'n' of 0.05 for (a) sodium and (b) potassium, with M_s of 1.5 for (c) sodium and (d) potassium and with M_s of 2.0 for (e) sodium and (f) potassium based mixes

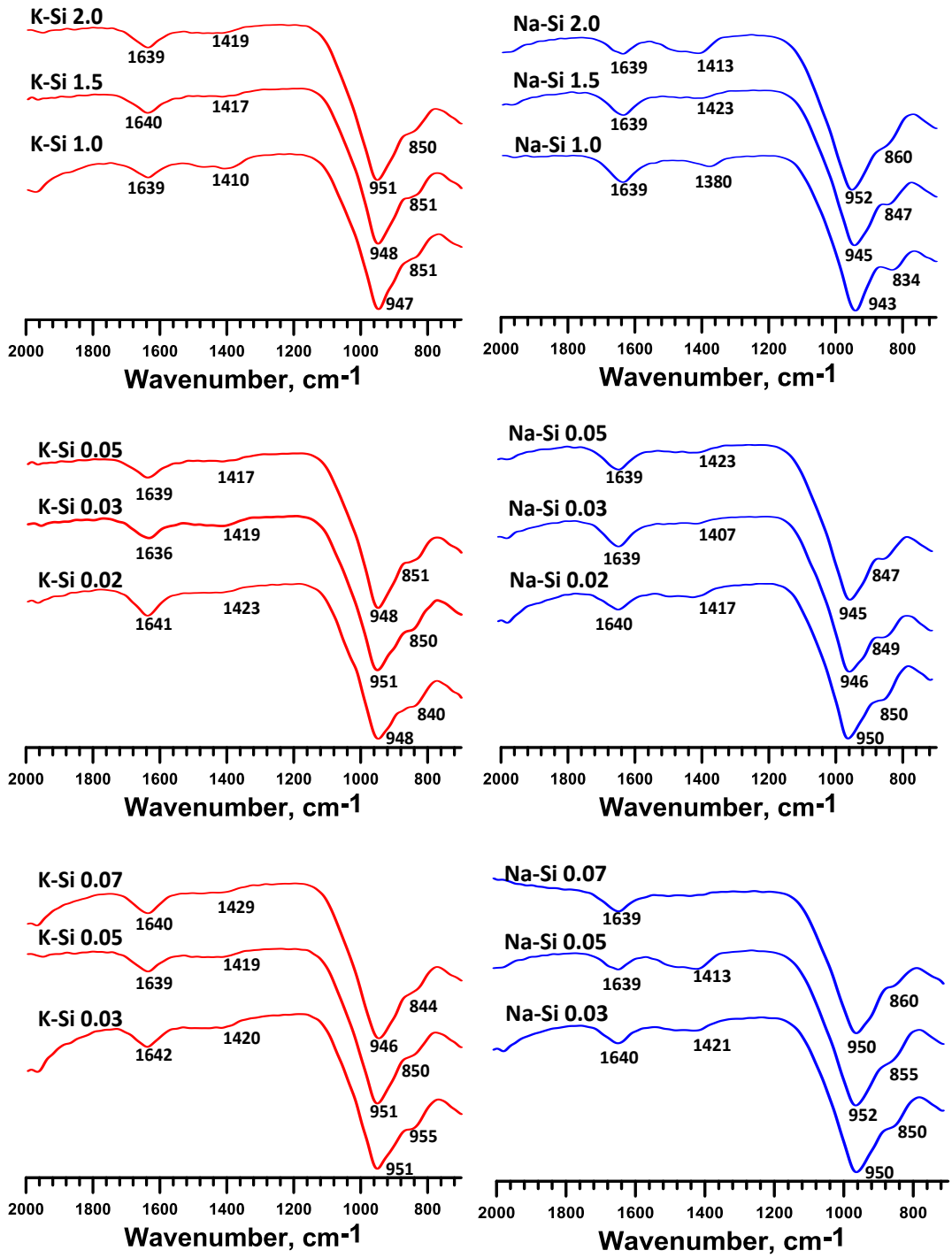

Figure 28: FTIR spectra for 7 day pastes with 'n' of 0.05 for (a) sodium and (b) potassium, with M_s of 1.5 for (c) sodium and (d) potassium and with M_s of 2.0 for (e) sodium and (f) potassium based mixes

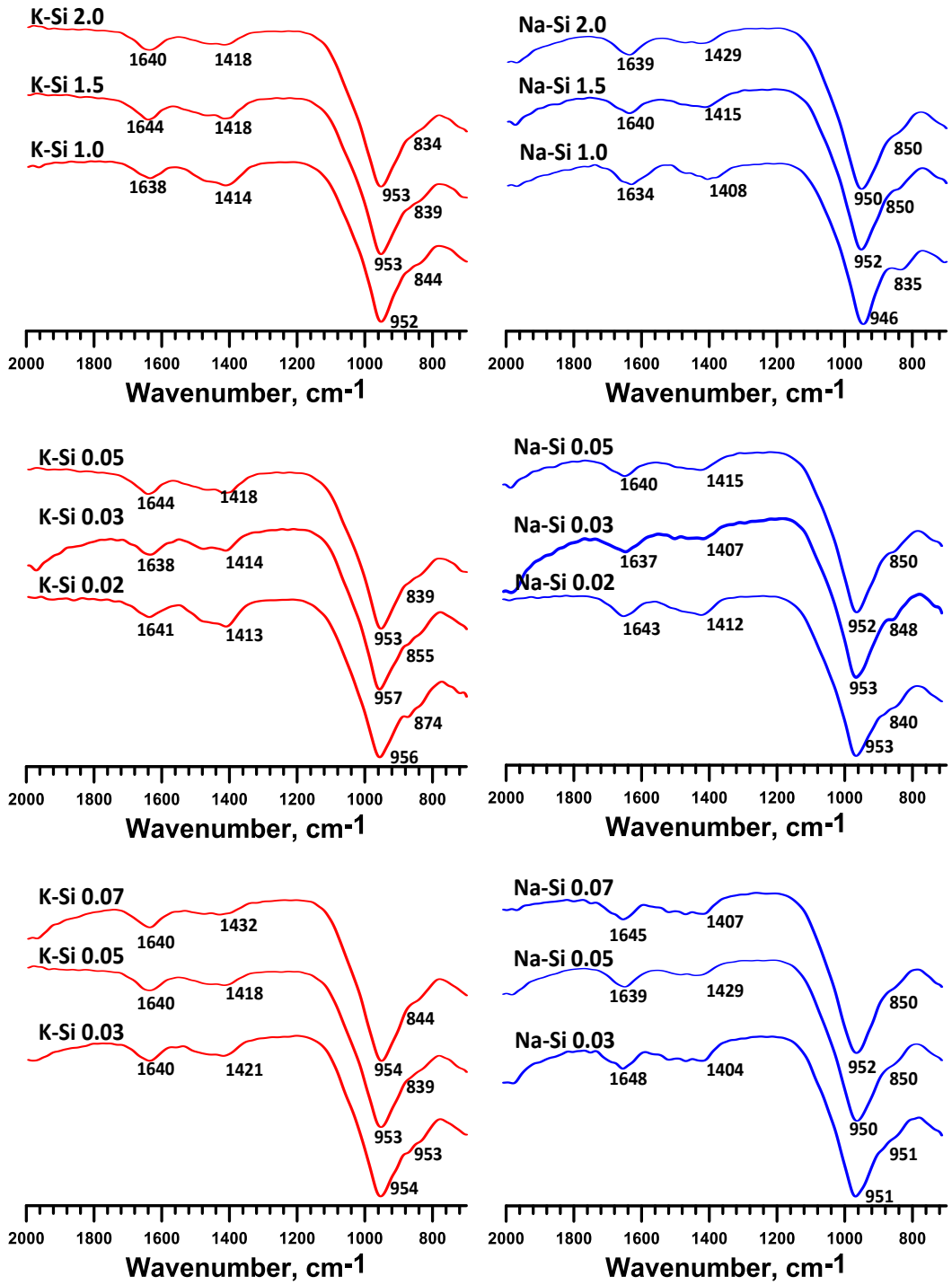

Figure 29: FTIR spectra for 28 day pastes with ‘n’ of 0.05 for (a) sodium and (b) potassium, with M_s of 1.5 for (c) sodium and (d) potassium and with M_s of 2.0 for (e) sodium and (f) potassium based mixes

The peaks associated with the vibrations of the asymmetric Si-O-Si tetrahedral (between 940-965 cm^{-1}) are generally indicative of the degree of polymerization that has taken place (van Jaarsveld and van Deventer, 1999), with higher wavenumbers being linked with higher degrees of polymerization. The values obtained are fairly similar although there seems to generally be a shift to higher wavenumbers in the case of the K-based binders. For these binders, the higher frequencies of the asymmetric vibrations of the Si-O-Si bonds could signify an increased degree of polycondensation due to the presence of potassium (van Jaarsveld and van Deventer, 1999). This also supports the compressive strength results discussed in earlier sections.

It is also interesting to note that for any given mix with constant binder composition and activator used, the peaks between 920-965 cm^{-1} seem to generally shift towards lower wavenumbers as the M_s ratios are decreased. The reason for this is an increasing number of Al substituting for Si as both the alkalinity and number of charge balancing ions increase (van Jaarsveld and van Deventer, 1999).

5.6 Summary

It was observed that the K-silicate activated slag pastes demonstrate higher heat of reaction after 72h. The induction period was shorter and the intensity of the acceleration peak higher for the K-silicate activated systems at lower M_s values than those activated with Na-silicate showing the effectiveness of K-based activators, including those contributed by the smaller solvated radius of K^+ in early-age reactions. Activator concentration increase led to a higher initial dissolution peaks for both Na and K-silicate pastes. However, solubility of Na-silicate powder activators was variable, affecting the acceleration phase of hydration as well. In K-silicate pastes activator concentration had no effect of the acceleration phase. Thus is can be concluded that M_s influences the acceleration phase greatly and the activator concentration affects the initial dissolution and the acceleration phase both based on the solubility of the silicate powder. The early-age compressive strength results also validate this observation. At later ages, the compressive strengths are higher for the K-silicate activated systems at higher activator concentration attributable to the effects of increased amounts of K that likely resulted in a more crystalline reaction product. Increasing the silica content of the activator resulted in comparable later-age strengths with negligible influence of the alkali cation type.

At later ages, the K-silicate activated pastes showed more reaction product from TG analysis corresponding to compressive strength data. The degree of polymerization determined using FTIR clearly indicates the non-polymerized silica at early ages, which then reaches higher degree of polymerization at later ages hinting at a more polymerized and dense structure. The activator being in powder form and insoluble in a free state, led to a slow diffusion especially in case of Na-silicate powder.

6. CONCLUSION

6.1 Influence of cation and externally added hydroxide on liquid alkali silicate and hydroxide activated slag.

The chief conclusions drawn in the study of liquid silicate activated slag on the strength and reaction products were as follows:

- For potassium silicate based mixtures gave high heat of reaction at the end of 72 hours. The induction period was shorter and the intensity of the acceleration peak was higher as compared to the sodium silicate mixes.
- At early ages the potassium silicate mixes gain strength but at later ages sodium silicate based mixes. The early age compressive strength gain conformed to the isothermal calorimetric results.
- Increasing the silica content of the activator resulted in comparable later age strengths irrespective of the alkali cation type.
- At lower M_s ratios, the compressive strength are higher due to better dissociation due to addition of hydroxide which allows for better polycondensation reaction.
- Hydrotalcite formation was observed for all the mixes at later age, followed by the decrease in the peak attributed to water loss.
- The reaction product or C-(A)-S-H gel formed is more for potassium silicate mixes at early ages and is more for the sodium silicate mixes at later ages. This also conforms to the compressive strength data.

- Silica polymerization is observed more in the sodium silicate mixes which can be attributed to the polarizing effect of the sodium ion to severe the silica bonds and form the dense polymeric chains during the polycondensation reaction.

6.2 Effect of cation on reaction kinetics and product formation in slag binders activated using alkali silicate powders and hydroxides

The main conclusions drawn in the study of the effect of activator characteristics on the reaction product formation in slag binders activated using alkali silicate powders and hydroxides were as follows:

- The results of this study indicate that the binders activated using potassium performs better than those activated using sodium at later ages. This can be attributed to a number of reasons; heat generated by the dissociation of the alkali activating powders into solution and the dissolution capabilities of the alkali activators.
- This can be related to the fact that Na-based activation solutions were not homogeneous and the solubility of the silicate powders was less with more addition of hydroxide.
- In the reaction kinetics it was observed that the initial dissolution peak is a function of activator concentration ‘n’ and the acceleration peak is the function of the M_s.
- The difference in the cation and ‘n’ is enhanced at a lower M_s and the compressive strengths are converged with effect of cation and M_s reduced.

- FTIR analysis of the hydrated pastes shows the effects of the silica modulus, with an increase in wavenumber resulting for an increase in M_s value of the activator. This is because an increasing number of Al substitutes for Si as both the alkalinity and number of charge balancing ions increase.
- There seems to be a general shift to higher wavenumbers in the case of the K-based binders. For these binders, the higher frequencies of the asymmetric vibrations of the Si-O-Si bonds could signify an increased degree of polycondensation due to the presence of potassium.

WORK CITED

1. Alonso, S., Palomo, A., 2001. Alkaline activation of metakaolin and calcium hydroxide mixtures: influence of temperature, activator concentration and solids ratio. Mater. Lett. 47, 55–62.

2. Altan, E., Erdoğan, S.T., 2012. Alkali activation of a slag at ambient and elevated temperatures. Cem. Concr. Compos. 34, 131–139.

3. Astutiningsih, S., Liu, Y., 2005. Geopolymerisation of Australian slag with effective dissolution by the alkali, in: Proceedings of the World Congress Geopolymer. pp. 69–73.

4. Bach, T.T.H., Chabas, E., Pochard, I., Cau Dit Coumes, C., Haas, J., Frizon, F., Nonat, A., 2013. Retention of alkali ions by hydrated low-pH cements: Mechanism and Na+/K+ selectivity. Cem. Concr. Res. 51, 14–21.

5. Bakharev, T., Sanjayan, J.G., Cheng, Y.-B., 1999. Effect of elevated temperature curing on properties of alkali-activated slag concrete. Cem. Concr. Res. 29, 1619–1625.

6. Ben Haha, M., Le Saout, G., Winnefeld, F., Lothenbach, B., 2011. Influence of activator type on hydration kinetics, hydrate assemblage and microstructural development of alkali activated blast-furnace slags. Cem. Concr. Res. 41, 301–310.

7. Bentz, D.P., Coveney, P.V., Garboczi, E.J., Kleyn, M.F., Stutzman, P.E., 1994. Cellular automaton simulations of cement hydration and microstructure development. Model. Simul. Mater. Sci. Eng. 2, 783.

8. Bernal, S.A., Mejía de Gutiérrez, R., Pedraza, A.L., Provis, J.L., Rodriguez, E.D., Delvasto, S., 2011. Effect of binder content on the performance of alkali-activated slag concretes. Cem. Concr. Res. 41, 1–8.

9. Cheerarot, R., Jaturapitakkul, C., 2004. A study of disposed fly ash from landfill to replace Portland cement. Waste Manag. 24, 701–709.

10. Chen, W., Brouwers, H.J.H., 2007. The hydration of slag, part 1: reaction models for alkali-activated slag. J. Mater. Sci. 42, 428–443.

11. Chithiraputhiran, S., Neithalath, N., 2013. Isothermal reaction kinetics and temperature dependence of alkali activation of slag, fly ash and their blends. Constr. Build. Mater. 45, 233–242.

12. Chithiraputhiran, S.R., 2012. Kinetics of Alkaline Activation of Slag and Fly ash-Slag Systems. Arizona State University, Tempe.

13. Choate, W.T., 2003. Energy and emission reduction opportunities for the cement industry.

14. Dakhane, A., Neithalath, N., Peng, Z., Marzke, R., n.d. The effects of cationic type (Na, K) on reaction kinetics and products of alkali activated slag. Constr. Build. Mater.

15. Davidovits, J., 1999. Chemistry of geopolymeric systems, terminology, in: Geopolymer. pp. 9–40.

16. Davidovits, J., 2005. Geopolymer chemistry and sustainable development. The poly (sialate) terminology: a very useful and simple model for the promotion and understanding of green-chemistry, in: Proceedings of the World Congress Geopolymer, Saint Quentin, France. pp. 9–15.

17. Depasse, J., 1997. Coagulation of Colloidal Silica by Alkaline Cations: Surface Dehydration or Interparticle Bridging? J. Colloid Interface Sci. 194, 260–262.

18. Depasse, J., 1999. Simple Experiments to Emphasize the Main Characteristics of the Coagulation of Silica Hydrosols by Alkaline Cations: Application to the Analysis of the Model of Colic et al. J. Colloid Interface Sci. 220, 174–176.

19. Dimas, D., Giannopoulou, I., Panias, D., 2009. Polymerization in sodium silicate solutions: a fundamental process in geopolymerization technology. J. Mater. Sci. 44, 3719–3730.

20. Duxson, P., Fernández-Jiménez, A., Provis, J.L., Lukey, G.C., Palomo, A., Deventer, J.S.J. van, 2007. Geopolymer technology: the current state of the art. J. Mater. Sci. 42, 2917–2933.

21. Fernandez-Jimenez, A., García-Lodeiro, I., Palomo, A., 2007. Durability of alkali-activated fly ash cementitious materials. J. Mater. Sci. 42, 3055–3065.

22. Fernandez-Jiménez, A., Palomo, A., Criado, M., 2006. A comparative study between sodium and potassium activators. Mater. Construccion 56, 51–65.

23. Fernández-Jiménez, A., Palomo, A., Sobrados, I., Sanz, J., 2006. The role played by the reactive alumina content in the alkaline activation of fly ashes. Microporous Mesoporous Mater. 91, 111–119.

24. Fernández-Jiménez, A., Puertas, F., Sobrados, I., Sanz, J., 2003. Structure of Calcium Silicate Hydrates Formed in Alkaline-Activated Slag: Influence of the Type of Alkaline Activator. J. Am. Ceram. Soc. 86, 1389–1394.

25. Fernández-Jiménez, A., Zibouche, F., Boudissa, N., García-Lodeiro, I., Abadlia, M.T., Palomo, A., 2013. “Metakaolin-Slag-Clinker Blends.” The Role of Na+ or K+ as Alkaline Activators of Theses Ternary Blends. J. Am. Ceram. Soc. 96, 1991–1998.

26. Garcia-Lodeiro, I., Fernández-Jimenez, A., Palomo, A., 2013. Hydration Kinetics in Hybrid Binders: Early Reaction Stages. Cem. Concr. Compos.

27. Glukhovsky, V.D., 1959. Soil silicates. Gostroiizdat Publ. Kiev USSR.

28. Glukhovsky, V.D., 1965. Soil silicates. Their properties, technology and manufacturing and fields of application, Doct. Tech. Sc. Degree Thesis. Civ. Eng. Inst. Kiev.

29. Glukhovsky, V.D., Rostovskaja, G.S., Rumyna, G.V., 1980. High strength slag-alkaline cements, in: 7th International Congress on the Chemistry of Cement. pp. 164–168.

30. Haha, M.B., Lothenbach, B., Le Saout, G., Winnefeld, F., 2012. Influence of slag chemistry on the hydration of alkali-activated blast-furnace slag — Part II: Effect of Al2O3. Cem. Concr. Res. 42, 74–83.

31. Hajimohammadi, A., Provis, J.L., van Deventer, J.S.J., 2011. The effect of silica availability on the mechanism of geopolymerisation. Cem. Concr. Res. 41, 210–216.

32. Hardjito, D., Rangan, B.V., 2005. Development and properties of low-calcium fly ash-based geopolymer concrete. Perth Aust. Curtin Univ. Technol.

33. Hong, S.-Y., Glasser, F.., 2002. Alkali sorption by C-S-H and C-A-S-H gels: Part II. Role of alumina. Cem. Concr. Res. 32, 1101–1111.

34. Khale, D., Chaudhary, R., 2007. Mechanism of geopolymerization and factors influencing its development: a review. J. Mater. Sci. 42, 729–746.

35. Krivenko, P.V., 1994. Alkaline cements. Alkaline Cem. Concr. 1, 11–129.

36. Lothenbach, B., Gruskovnjak, A., 2007. Hydration of alkali-activated slag: thermodynamic modelling. Adv. Cem. Res. 19, 81–92.

37. Mahasenan, N., Smith, S., Humphreys, K., Kaya, Y., 2003. The cement industry and global climate change: current and potential future cement industry CO2 emissions, in: Greenhouse Gas Control Technologies-6th International Conference. Oxford: Pergamon. pp. 995–1000.

38. McDonald, M., Thompson, J.L., 2003. Sodium silicate a binder for the 21st century. Ind. Chem. Div. PQ Corp.

39. Palacios, M., Puertas, F., 2006. Effect of Carbonation on Alkali-Activated Slag Paste. J. Am. Ceram. Soc. 89, 3211–3221.

40. Palomo, A., Fernández-Jiménez, A., Kovalchuk, G., Ordoñez, L.M., Naranjo, M.C., 2007. Opc-fly ash cementitious systems: study of gel binders produced during alkaline hydration. J. Mater. Sci. 42, 2958–2966.

41. Phair, J.W., Van Deventer, J.S.J., 2001. Effect of silicate activator pH on the leaching and material characteristics of waste-based inorganic polymers. Miner. Eng. 14, 289–304.

42. Provis, J.L., van Deventer, J.S.J., 2007. Geopolymerisation kinetics. 1. In situ energy-dispersive X-ray diffractometry. Chem. Eng. Sci. 62, 2309–2317.

43. Puertas, F., Fernández-Jiménez, A., 2001. Setting of alkali-activated slag cement. Influence of activator nature. Adv. Cem. Res. 13, 115–121.

44. Puertas, F., Fernández-Jiménez, A., 2003. Mineralogical and microstructural characterisation of alkali-activated fly ash/slag pastes. Cem. Concr. Compos. 25, 287–292.

45. Puertas, F., Fernández-Jiménez, A., Blanco-Varela, M.., 2004. Pore solution in alkali-activated slag cement pastes. Relation to the composition and structure of calcium silicate hydrate. Cem. Concr. Res. 34, 139–148.

46. Purdon, A.O., 1940. The action of alkalis on blast-furnace slag. J. Soc. Chem. Ind. 59, 191–202.

47. Rangan, B.V., 2008. Fly ash-based geopolymer concrete. Your Build. Adm. 2.

48. Ravikumar, D., 2012. Property development, microstructure and performance of alkali activated fly ash and slag systems. Clarkson University.

49. Ravikumar, D., Neithalath, N., 2012a. Effects of activator characteristics on the reaction product formation in slag binders activated using alkali silicate powder and NaOH. Cem. Concr. Compos. 34, 809–818.

50. Ravikumar, D., Neithalath, N., 2012b. Reaction kinetics in sodium silicate powder and liquid activated slag binders evaluated using isothermal calorimetry. Thermochim. Acta 546, 32–43.

51. Roy, D.M., 1999. Alkali-activated cements Opportunities and challenges. Cem. Concr. Res. 29, 249–254.

52. Saeed, A., Hammons, M.I., Petermann, J.C., 2010. Alkali-Activated Geopolymers: A Literature Review. APPLIED RESEARCH ASSOCIATES INC PANAMA CITY FL.

53. Schneider, J., Cincotto, M.., Panepucci, H., 2001. 29Si and 27Al high-resolution NMR characterization of calcium silicate hydrate phases in activated blast-furnace slag pastes. Cem. Concr. Res. 31, 993–1001.

54. Shi, C., Day, R.L., 1995. A calorimetric study of early hydration of alkali-slag cements. Cem. Concr. Res. 25, 1333–1346.

55. Song, S., Sohn, D., Jennings, H.M., Mason, T.O., 2000. Hydration of alkali-activated ground granulated blast furnace slag. J. Mater. Sci. 35, 249–257.

56. Vail, J.G., Wills, J.U., 1952. Soluble Silicates: Their Properties And Uses, Vol. 2: Technology.

57. Van Jaarsveld, J.G.., van Deventer, J.S.., 1999. The effect of metal contaminants on the formation and properties of waste-based geopolymers. Cem. Concr. Res. 29, 1189–1200.

58. Van Jaarsveld, J.G.., van Deventer, J.S.., Lukey, G.., 2002. The effect of composition and temperature on the properties of fly ash- and kaolinite-based geopolymers. Chem. Eng. J. 89, 63–73.

59. Vance, K., Dakhane, A., Neithalath, N., n.d. Rheological behaviour of alkali activated fly ash suspensions: Influence of the activator type and chemistry.

60. Wadsö, L., 2003. An experimental comparison between isothermal calorimetry, semi-adiabatic calorimetry and solution calorimetry for the study of cement hydration. Nord. Rep. TR 522.

61. Wang, S.-D., Scrivener, K.L., 1995. Hydration products of alkali activated slag cement. Cem. Concr. Res. 25, 561–571.

62. Wang, S.-D., Scrivener, K.L., Pratt, P.L., 1994. Factors affecting the strength of alkali-activated slag. Cem. Concr. Res. 24, 1033–1043.

62. Yip, C.K., Lukey, G.C., van Deventer, J.S.J., 2005. The coexistence of geopolymeric gel and calcium silicate hydrate at the early stage of alkaline activation. Cem. Concr. Res. 35, 1688–1697.

63. Živica, V., 2007. Effects of type and dosage of alkaline activator and temperature on the properties of alkali-activated slag mixtures. Constr. Build. Mater. 21, 1463–1469.